Self-assembly: from crystals to cells†

Bartosz A. Grzybowski,* Christopher E. Wilmer, Jiwon Kim, Kevin P. Browne and Kyle J. M. Bishop

Received 30th October 2008, Accepted 8th December 2008
First published as an Advance Article on the web 18th February 2009
DOI: 10.1039/b819321p

Self-assembly (SA) is the process in which a system's components—be it molecules, polymers, colloids, or macroscopic particles—organize into ordered and/or functional structures without human intervention. The main challenge in SA research is the ability to "program" the properties of the individual pieces such that they organize into a desired structure. Although a general strategy for doing so is still elusive, heuristic rules can be formulated that guide design of SA under various conditions and thermodynamic constraints. This Review examines SA in both the equilibrium and non-equilibrium/dynamic systems and discusses different SA modalities: energy driven, entropy-driven, templated, and field-directed. Non-equilibrium SA is discussed as a route to reconfigurable ("adaptive") materials, and its connection to biological systems is emphasized.

1. Introduction

Self-assembly (SA) is the ultimate dream of a lazy scientist: just mix the components, and the forces of nature will assemble them into a desired structure. Over the past several decades, the appeal of this vision has motivated countless chemists, physicists, and engineers to construct self-assembling systems at scales from the molecular to the macroscopic. This effort has met with considerable success. In molecular sciences, SA provides the basis for crystallization of organic[1,2] and inorganic[3,4] molecules and is at the heart of supramolecular chemistry,[5,6] where the "instructions" of how to assemble larger entities are "coded" in the structural motifs of individual molecules. In nanotechnology, SA underlies various types of molecular structures (*e.g.*, Langmuir-Blodgett films,[7] self-assembled monolayers,[8–10] amphiphilic fibers[11,12]) as well as higher-order architectures built from nanoparticles,[13–16] nanotubes,[17] or nanorods.[18] At the microscale, there are currently self-assembling fluidic machines[19] and micromixers,[20] complex microparticles building themselves from prepolymer patches,[21] and artificial opals comprising millions of colloidal particles.[22,23] Some of the macroscopic manifestations of SA include 2D and 3D structures driven by capillary forces,[24,25] self-assembling electronic circuits,[26,27] and unusual crystals of charged components.[28,29] Some of the SA strategies are already finding industrial applications. For example, Alien Technologies has developed fluidic self-assembly methods to fabricate radio-frequency identification (RFID) tags, by using shape recognition and fluid transport on the microscale.[30,31]

Department of Chemistry, Department of Chemical and Biological Engineering, Northwestern University, 2145 Sheridan Road, Evanston, 60208, USA. E-mail: grzybor@northwestern.edu

† This paper is part of a *Soft Matter* theme issue on Self-Assembly. Guest editor: Bartosz Grzybowski.

Bartosz A. Grzybowski

Bartosz A. Grzybowski graduated in Chemistry from Yale University in 1995. He obtained his PhD in Physical Chemistry from Harvard University in 2000 (with G. M. Whitesides). In 2003 he joined the faculty of Northwestern University where he is now an Associate Professor of Chemical and Biological Engineering and Chemistry. His scientific interests include self-assembly in non-equilibrium/dynamic systems, complex chemical networks, nanostructured materials and nanobiology. He is a recipient of the NSF CAREER, the American Chemical Society Unilever, and the Gerhard Kanig Innovation Award, and has been named a Pew Scholar in the Biomedical Sciences, Alfred P. Sloan Fellow, and Dreyfus Teacher-Scholar.

Christopher E. Wilmer

Christopher E. Wilmer graduated from the University of Toronto in 2007 with a BS in Engineering Science. He is currently a PhD candidate with Prof. Bartosz A. Grzybowski in the Department of Chemical and Biological Engineering at Northwestern University. His research interests lie in the theory of static and dynamic self-assembly, periodic pattern formation, applications of graph theory to organic chemistry, and the role of folding-problems (origami) in designing self-assembling nanosystems. He is currently investigating geometrical effects on the electrostatic self-assembly of charged objects at the nanoscale.

Nanogen employs electric-field mediated self-assembly to bring together DNA nanocomponents for electronic and diagnostic devices.[32] IBM, too, has recently harnessed the power of SA to create trillions of nanometre-sized holes across the length of a 300 millimetre computer chip, thus creating new insulators that increase the speed (by 35%) and efficiency (by 15%) of electrical signal transmission.[33]

In many of the above examples, SA capitalizes on the fact that with the current state of chemistry/material science it is often easier to fine tune the interparticle forces that bring small components together than to manipulate or modify these components by optical tweezers,[34] atomic traps,[35] or other high-end techniques. Of course, this is not always the case, and "programming" the correct interactions into self-assembling molecules or particles is often based on intuition rather than predictive formulas. Consequently, identification of reverse-engineering strategies that would identify the necessary interactions required for a specific mode of SA is one of the holy grails of SA research (see article by Torquato later in this issue).

But there are even more challenging problems—nay, opportunities!—on the horizon. Despite all the impressive demonstrations of SA, we are still very far from using it as flexibly and creatively as nature does. In the vast majority of man-engineered SA systems, the structures that emerge are ordered but static—once made, they cannot be further adjusted/reconfigured and cannot perform different functions depending on the changes in external parameters. They are "crystals" not "cells." In cells, tissues, and organisms, SA builds *dynamic* aggregates that change and function outside the confines of thermodynamic equilibria: transcriptional machinery that replicates DNA, fibers comprising the cytoskeleton, and motors powering bacteria are just a few of the many examples. These and other dynamic self-assembling systems could provide the basis for adaptive, self-replicating, or self-healing materials of the future. Unfortunately, we still know precious little about the principles governing SA away from equilibrium or even about the heuristic rules for the design of such systems.

This Tutorial Review is an attempt to summarize and systematize what we know and what we do not know about SA and also to discuss the future of self-assembly research. Since the field is so diverse, we will be able to discuss only the key issues and most representative systems in both the equilibrium and non-equilibrium regimes. Before doing so, however, let us first codify what is actually understood by self-assembly.

2. Definitions

The existing definitions of SA appear to be so creatively diverse—to the point of cliché—that in their classic 2002 paper, Whitesides and Grzybowski asked a rather provocative question: "Is anything *not* self-assembly?" Indeed, non-covalent association of molecules, aggregation of small particles, and the growth of quantum dots have all been, at some point, termed self-assembly. Are two molecules undergoing a chemical reaction also self-assembling? Or two water droplets merging together? Clearly, we need some more precision here. Looking into Webster's dictionary, we learn that *assembly* is the process of "fitting together of manufactured parts into a complete machine, structure, or unit of a machine". The key words here are "parts" (*i.e.*, discrete and manufactured such that their shape/properties matter) and "fitting together" (implying some spatial ordering).

Jiwon Kim

Jiwon Kim graduated in Chemistry from Korea Advanced Institute of Science and Technology in 2006, and worked in the Synthetic and Medicinal Laboratory at Seoul National University from 2006 to 2007. She is currently a PhD candidate working with Prof. Bartosz A. Grzybowski in the department of Chemistry at Northwestern University. Her research focuses on the synthesis of nanomaterials which have a wide range of applications and development of chemical systems based on dynamic self-assembly.

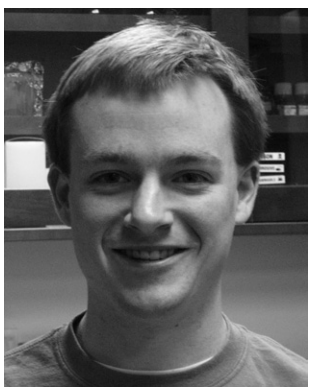

Kevin P. Browne

Kevin P. Browne received his undergraduate degree from Georgetown University in 2008. He is currently a PhD candidate with Prof. Bartosz Grzybowski in the Department of Chemistry at Northwestern University. His interests lie in the synthesis of photo-switchable chemical systems and the dynamic spatial regulation of discrete nanoscale components using the tools of organic and inorganic chemistry.

Kyle J. M. Bishop

Kyle J. M. Bishop graduated from the University of Virginia in 2003 with a B.S. in Chemical Engineering. He is currently a PhD candidate working with Prof. Bartosz Grzybowski in the department of Chemical and Biological Engineering at Northwestern University. His research interests include nanoscale electrostatics and self-assembly, complex chemical reaction networks, and pattern formation in reaction-diffusion systems. He is an NSF Graduate Fellow.

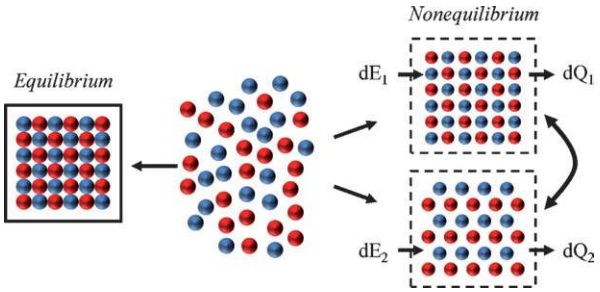

Fig. 1 A scheme highlighting the differences between equilibrium and non-equilibrium/dynamic self-assembly. In the former, particles form a "static" structure closed to energy exchange with environment. In the latter, the flux of energy through the system (later dissipated as heat), maintains an organized assembly in one of several metastable states. For different rates of energy input (dE_1 vs. dE_2), different structures may form under DySA.

Following this logic, we propose to define self-assembly as the spontaneous formation of *organized* structures from many *discrete* components that interact with one another directly (*e.g.*, by electrostatic repulsions[36]) and/or indirectly, through their environment (*e.g.*, magnetohydrodynamic SA,[37,38] *cf.* Section 8). The term "organized" refers to some form of spatial and/or temporal ordering (*e.g.*, an ionic crystal) and distinguishes SA proper from less ordered aggregation processes such as precipitation[39] and ballistic deposition.[40] Furthermore, because the building blocks of SA structures are specified as "discrete," our definition excludes pattern formation in continuous media such as Bénard convection,[41,42] chemical waves,[43–45] and Turing structures,[46,47] where the knowledge of the shapes/identities of individual particles/molecules is not important in the description of the phenomenon.

Within this conceptual framework, we make a further distinction between equilibrium self-assembly (ESA) and dynamic self-assembly (DySA) by considering the thermodynamic description of the resulting assemblies (Fig. 1). ESA refers to stable *equilibrium* structures characterized by a maximum (local or global) in the system's entropy and no systematic energy flows. Examples include organic[1,2] and inorganic crystals,[3,4] block copolymer assemblies,[48,49] supramolecular structures,[5,6,50] and capillary SA.[51,52] In contrast, DySA refers to ordered *non-equilibrium* structures, which are maintained far from equilibrium by a supply and subsequent dissipation (*e.g.*, into heat) of useful energy. Free from the constraints of entropy maximization, these systems can "reside" in low entropy states often characterized by complex spatial or coherent spatio-temporal organization. Furthermore, the variety of dissipative interactions (*cf.* Table 3) and the dependence of DySA systems on an external energy supply provide a basis for the systematic design and control of synthetic DySA systems (see Section 8).

3. ESA and thermodynamics

At thermodynamic equilibrium, SA evolves the system's components into a structure that corresponds to the minimum of an appropriate thermodynamic potential. This potential is determined by the thermodynamic parameters that are held constant during the process. For instance, if temperature, T, pressure, P, and the number of molecules, N, in the system do not change, self-assembly tends to the minimum of the Gibbs free energy, $G = H - TS$ (H is the enthalpy, S is the entropy), whose changes, $\Delta G = \Delta H - T\Delta S$, determine the spontaneity of the process (spontaneous if $\Delta G < 0$). In another common situation, when T, V (volume of the system) and N are kept constant, the self-assembled state is given by the minimum of the Helmholtz free energy, $F = U - TS$ (where U is the internal energy), with the process being spontaneous if $\Delta F = \Delta U - T\Delta S < 0$. The important insight here is that SA can be due to either enthalpic/energetic effects (*e.g.*, ΔH or $\Delta U < 0$, $\Delta S \approx 0$), entropic effects (ΔH or $\Delta U \approx 0$, $\Delta S > 0$), or both. Let us review some illustrative examples.

3.1. ESA driven by energetics

Consider a system comprising two types of macroscopic, polymeric spheres placed in a small dish.[28] When the dish is agitated

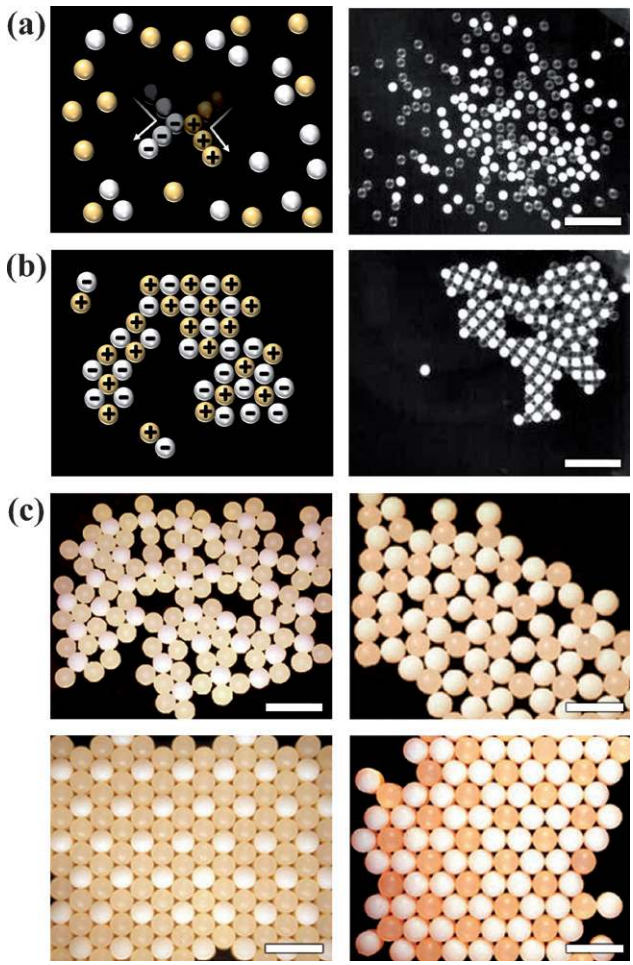

Fig. 2 Self-assembly by contact electrification. (a and b) The schemes (left column) and experimental images (right column) of the crystallizing spheres (here, Teflon—white and PMMA—clear). Collisions between spheres results in charge separation with spheres of one type becoming negatively charged and those of the other type, positively charged. (c) Four different lattice structures assembling from different relative numbers of Teflon and Nylon-6,6 spheres. Note the pentagonal, "quasi-crystalline" ordering in the structures in the top row. Scale bars are 10 mm. Images in (c) are adapted from ref. 28.

mechanically, the spheres roll on its surface and collide with one another. With the appropriate choice of materials (*e.g.*, Teflon, *A*, and PMMA, *B*), collisions between spheres *A* and *B* result in so-called contact electrification,[53–55] in which the two types acquire opposite electrical charges (*e.g.*, Teflon charges negatively; PMMA positively). The charged beads then begin to interact by electrostatic forces that mediate their self-assembly into various types of two-dimensional crystals and even quasi-crystals (Fig. 2).

Although, formally, this is a non-equilibrium system, the energy dissipated through the inelastic particle collisions is balanced by a steady influx of energy due to the random agitation of the dish. This external agitation acts as a macroscopic "thermostat," which maintains the average energy of the system—just as a thermal reservoir maintains the average internal energy of a microscopic system. Consequently, one can approximate the SA process as an equilibrium one and apply the thermodynamic concepts of entropy and free energy (here, Helmholtz's *F*).

Initially, the spheres have no charge and the potential energy of particle–particle interactions is negligible, $U_i \approx 0$. The spheres moving in the dish behave akin to a two-dimensional ideal gas, whose entropy is positive, $S_i > 0$ and can be approximated by $S_i \approx Nk_B[\ln(A/N\Lambda^2) + 1]$, where N is the number of spheres, A is the area of the surface available to the spheres, k_B is Boltzmann's constant, and Λ is the thermal de Broglie wavelength. In the final state, when all of the components are fully charged and assembled, the energy of the crystal is given by[28]

$$U_f = \sum_{i>j} \frac{Q_i Q_j}{r_{ij}} - \left(\frac{\varepsilon_i - 1}{\varepsilon_i + 2} + \frac{\varepsilon_j - 1}{\varepsilon_j + 2}\right)\frac{a^3 Q_i^2}{r_{ij}^4}$$

where Q is the electric charge, r is the interparticle distance, ε is the dielectric constant, a is the radius of the sphere, and the summation over all sphere pairs (i,j) accounts for the charge-charge interactions as well as the interactions between charges and charge-induced dipoles on neighboring spheres. The important thing to note is that this energy is favorable, $U_f < 0$ (for a typical crystal of 100 spheres, each charged to 0.3 nC, $U_f \approx -0.04$ mJ). At the same time, the entropy of the system is now reduced to that of one "super-particle" (*i.e.*, the entire crystal), $S_f \approx k_B[\ln(AN/\Lambda^2) + 1]$, which is much smaller than S_i, provided that the distance between the beads in the initial state is sufficiently large to apply the ideal gas approximation.

Overall, the entropic term in the free energy equation is unfavorable, $-T\Delta S > 0$, and it is the highly favorable energetic change, $\Delta U < 0$, that renders SA spontaneous, $\Delta F < 0$.

3.2. ESA driven by entropy

Equilibrium self-assembly driven entirely by entropy might seem somewhat mysterious. After all, isn't a system assembling spontaneously from a disordered state into an ordered one violating the second law of thermodynamics? Not necessarily. The classic example of entropy-driven SA systems are collections of elongated rods such as rigid liquid-crystal molecules,[56] colloidal particles,[56] or even viruses,[57] for which attractive interparticle interactions are negligible (Fig. 3). Entropic ordering in these systems had been predicted by Onsager,[58] but many critics later questioned whether in the experimental systems the rods do not interact with one another. The

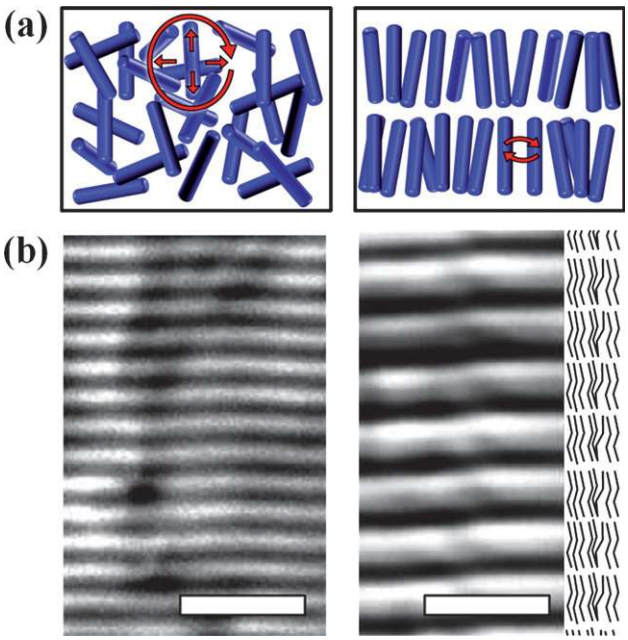

Fig. 3 (a) Spontaneous ordering of hard rods driven by entropy. In the disordered phase, the ability of the rods to twist and turn is hampered by interparticle collisions. The ordered state allows the rods to migrate through the layers more freely and so has *higher* entropy than the disordered phase. (b) Images of ordered, smectic phases formed by mutants of the bacteriophage virus, fd. In the left picture, the length of each virus is 0.64 μm; in the right picture, it is 1.2 μm. Scale bars are 4 μm. Images reproduced with permission from ref. 163. Copyright Wiley-VCH Verlag GmbH & Co. KGaA.

convincing proof that SA cannot possibly be driven by energetic effects is based on the experiments with like-charged rods,[59] which form ordered phases even though the electrostatic forces in the system are all repulsive. The origin of the mystery is explained in Fig. 3 and has to do with a prevalent misconception about entropy, which is not, as often expounded, about disorder but rather about the available degrees of freedom (and the volume of accessible phase space)! In the case of disordered rods, their rotations and translations are not really as free as they might seem since the rods bump against one another. When the rods orient into layers (the so-called smectic phase), they give up the ability to rotate and translate vertically but compensate these restrictions by the ability to diffuse more freely within the layer. Exact calculations show that the net effect of ordering is entropically favorable, $\Delta S = S_{ordered} - S_{disordered} > 0$. Therefore, even though $\Delta U \approx 0$, we have $\Delta F < 0$.

3.3. ESA driven by both enthalpy and entropy

This is by far the most common scenario for SA at the molecular and macro scales, where entropy of the molecules is usually commensurate with the magnitude of the non-covalent interparticle forces. SA of molecular crystals discussed in Section 4 is one example, micellization of dimeric surfactants[60] composed of two hydrophobic tails and a gemini cationic head ($[C_mH_{2m+1}(CH_3)_2N–(CH_2)_k–N(CH_3)_2C_nH_{2n+1}]Br_2$; Fig. 4) is another. For traditional, monomeric surfactants (*e.g.*, $[(CH_2)_3–NC_nH_{2n+1})]Br$), the process of self-assembly in water is

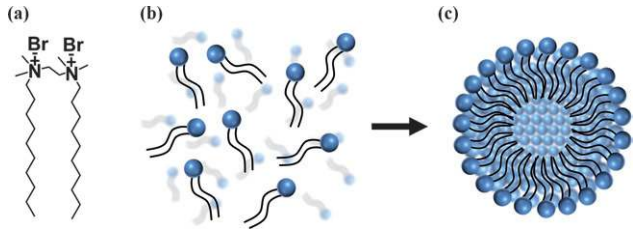

Fig. 4 (a) A typical dimeric surfactant composed of two hydrophobic tails and a gemini cationic head ($[C_mH_{2m+1}(CH_3)_2N–(CH_2)_k–N(CH_3)_2C_nH_{2n+1}]Br_2$; here, m = 10; n = 10; k = 2). (b and c) Dimeric surfactants self-assemble into micelles due to van der Waals and hydrophobic forces between the tails. Self-assembly is driven by both entropy and energy.

predominantly driven by entropy through the liberation of water from around the molecules' non-polar tails.[61] For dimeric surfactants, however, the van der Waals and hydrophobic forces between the tails of each molecule become dominant, and free energy changes, ΔG_{mic}, are mostly to be due to the enthalpic effects, $\Delta H_{mic} < 0$. In a series of meticulous calorimetric experiments, Thomas and co-workers[62] were able to show that whereas for $[C_{12}H_{25}(CH_3)_2N–(CH_2)_6]Br$ enthalpic changes contribute only 3.4% to the overall ΔG_{mic}, this percentage contribution increases to 61% of ΔG_{mic} when the dimeric surfactant, $[C_{12}H_{25}(CH_3)_2N–(CH_2)_{12}–N(CH_3)_2C_{12}H_{25}]Br_2$, is used. This example is quite instructive as an illustration of how even relatively small architectural changes (here, dimerization of surfactant monomers) can tip the balance between enthalpy and entropy quite dramatically. Yet, the micelles that form from monomeric and dimeric surfactants of the same tail lengths are virtually identical—does this mean that the outcome of SA is robust against changes in the component properties? And if it is robust, can it be easily predicted *a priori*? This brings us to the question of rational design of SA systems.

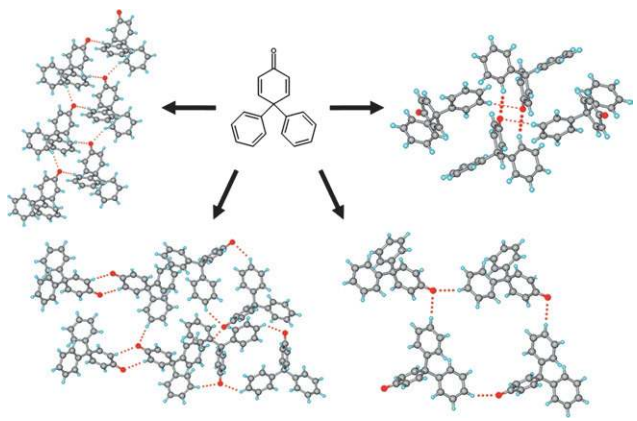

Fig. 5 An example of polymorphism in molecular crystals. 4,4-Diphenyl-2,5-cyclohexadienone is an example of a molecule that can crystallize into several different polymorphs (here, four are shown) from similar solvent mixtures. Adapted by permission from ref. 164. Copyright 2008 American Chemical Society.

4. Rational design and heuristics of ESA

Depending on the nature of the components, the ability to predict a self-assembled structure can be a relatively simple or quite an intractable problem. On one end of the spectrum are systems in which the components are highly symmetric and interact by simple potentials. In such cases, SA usually forms the same final structure that can sometimes be "guessed" intuitively—for instance, for the ensembles of microscopic latex beads interacting by all-attractive van der Waals forces, the final structure is almost always a hexagonally close-packed crystal. In sharp contrast, organic molecules interacting through multiple, non-covalent interactions (*e.g.*, hydrogen-bonding, van der Waals forces, electrostatic forces) of similar magnitudes can evolve, under identical experimental conditions, into as many as 10 "polymorphic" assemblies[63] (Fig. 5). In cases like this one, no rule-of-thumb predictions are possible, and even the most sophisticated computational tools currently available[1,2,64] are often insufficient to make correct *a priori* predictions. The good news for experimentalists working on SA is that theory has not yet rendered us useless, and for most non-trivial self-assembling systems experiments precede the theory. While the theory is in the making, one would like to develop at least some heuristic rules and intuition for designing components that self-assemble efficiently and at least somewhat predictably. Here are some characteristic "ingredients" for SA that one should consider:

4.1. Agitation and reversibility

The first, obvious, "rule" is that the components of the system should be agitated—at small scales simply by the inherent

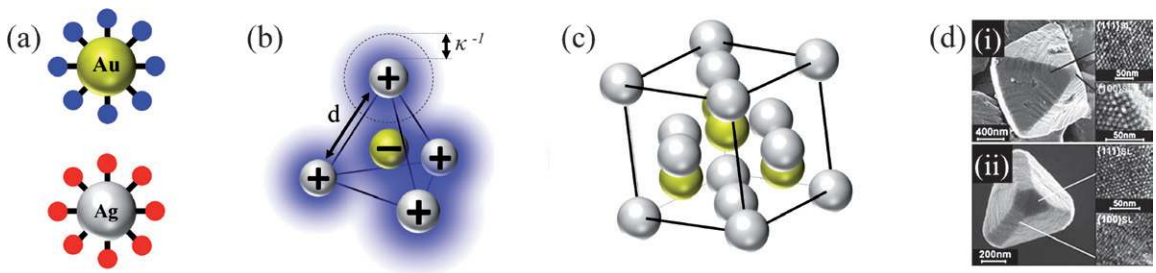

Fig. 6 "Programming" SA by specific interactions. (a–c) Oppositely charged nanoparticles (covered with $HS(CH_2)_{10}COO–$ and $HS(CH_2)_{11}NMe_3^+$ thiols) assemble into diamond-like crystals. This low-packing-fraction lattice forms as the result of a subtle interplay between charge-charge attractions and counterion screening, which minimizes repulsions between like-charged NPs by "pushing" these NPs apart. Counterion "atmospheres" in (b) are indicated by blue halos; κ^{-1} denotes the thickness of the Debye screening layer. (c) shows a unit cell of the forming crystals; (d) shows SEM images of the NP assemblies. Images in (d) are reproduced with permission from AAAS from Ref. 16.

thermal noise, and at larger scales by external means. Without agitation, the pieces can certainly clump together, but they are very unlikely to correct the defects and develop perfect order. Proper agitation can render the process reversible such that the pieces can come on and off the assembling structure and overcome local energetic minima that trap the self-assembly process. An interesting twist to this story is that agitation is usually most difficult to achieve at the scale of tens to hundreds of microns, especially if the particles are made of light-weight materials. In this regime, the effect of thermal noise is already small, while the external agitation by shaking, sound waves, etc. is often inefficient to impart the inertia (which scales with particle's mass) necessary to overcome strong surface forces (which scale with a particle's surface area). Agitation under these conditions becomes like shaking dust particles—that is, difficult—and one should think of eliminating the problem by minimizing the unwanted surface forces (by appropriate surface modification,[14,65] immersion in a fluid minimizing hydrophobic contrast[66,67]) to relieve the problem.

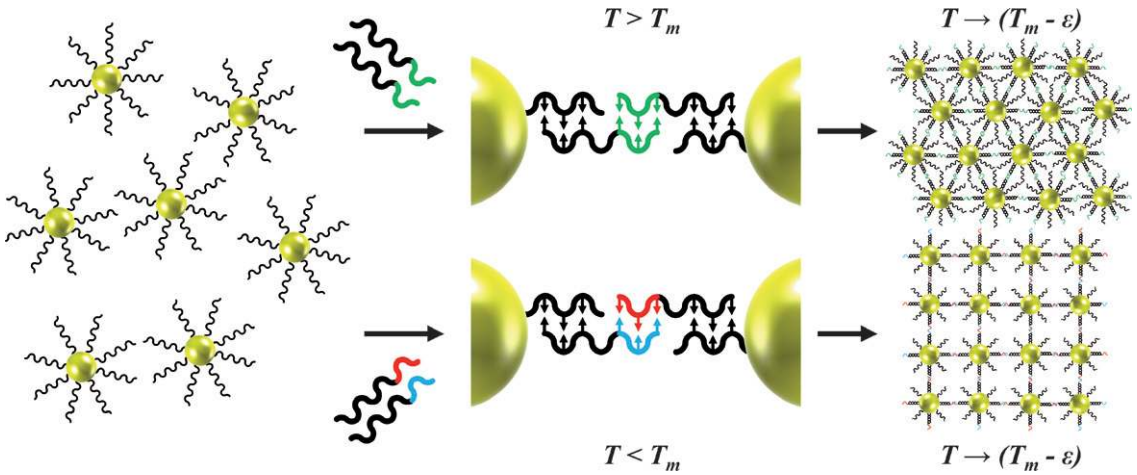

Fig. 7 Au nanoparticles functionalized with DNA can self-assemble specifically by addition of complimentary DNA with sequence-specific "linkers". (Top) In the simplest example, DNA (black and green) first binds to complementary strands (black) tethered onto the NP surfaces, thereby exposing a short "linker" sequence (green; *e.g.*, GCGC) to other, similarly functionalized AuNPs. These linkers then bind the particles together into an ordered structure *via* complementary base-pair interactions. The strength of these base-pair interactions can be modulated by changing the temperature of the system: above the melting temperature, T_m, particles are free in solution; for $T < T_m$, they organize into an ordered close-packed lattice. (Bottom) More complex structures can be created by the introduction of two types of NPs, each functionalized with a different "linker" sequence (red and blue) that bind specifically to one another (*e.g.*, red-blue but not red-red or blue-blue). In this case, introduction of an additional interaction leads to a different ordered structure. The scheme is based on the work of Mirkin *et al.*, ref. 71.

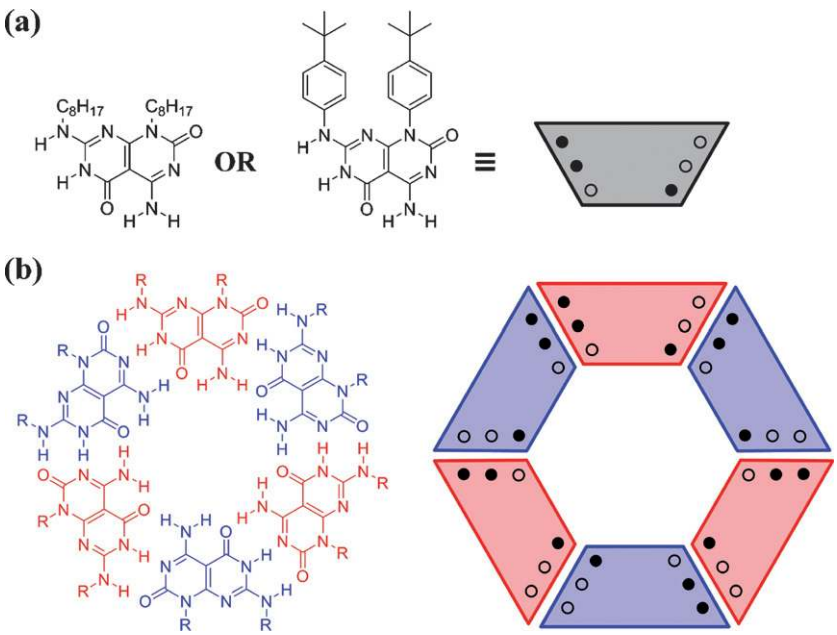

Fig. 8 Self-assembly of (a) self-complementary heterocycles into (b) macromolecular "rosettes". Schematic and structural representations are shown; ○ = hydrogen-bond acceptor; ● = hydrogen-bond donor; colors are used only for clarity. Inspired by Lehn *et al.*, ref. 73.

4.2. Specificity

An astute self-assembler should be able to operate with *specific* interactions. If all components attract indiscriminately, the pieces will form only the "trivial," close-packed assemblies (unless entropic effects of appreciable magnitude are added, see Section 3.2). Most interesting SA structures rely on specific recognition between different types of components. A simple manifestation of specificity at the nanoscale are crystals formed by oppositely charged nanoparticles[16,68,69] where only the oppositely charged NPs attract while the like-charged NPs try to stay apart. The subtle interplay between these tendencies and some interesting counterion effects[70] can then evolve the NPs into large crystals characterized by diamond packing (*i.e.*, a lattice of the lowest known packing fraction) (Fig. 6). A more complex nanoscopic system is Mirkin's nanoparticles covered with short DNA strands.[71] During self-assembly, only the complimentary strands recognize one another, and the NPs form crystals of desired lattice types (Fig. 7).

4.3. Directionality

Specificity is often related to the *directionality* of interactions. One class of systems we already mentioned are molecular crystals, in which directional interactions such as hydrogen-bonding can organize the molecules into intricate supramolecular architectures (Fig. 8).[72–75] If properly engineered into the system, directionality can extend to length scales far greater that those of the components. A beautiful example here is Stupp's nanofibers made of amphiphilic molecules comprising hydrophobic "tails" and appropriately crafted peptide "heads" (Fig. 9).[11,12] Similar to traditional surfactants, these molecules assemble in water so as to bury the tails and expose the heads. Instead of forming spherical micelles, however, the peptides prefer to hydrogen-bond into planar β-sheets, and the amphiphiles organize into micron-long cylinders.[76] In other words, the local directionality of hydrogen-bonding between neighboring molecules translates into large-scale directionality of the self-assembled structures. The regularity and robustness of the fibers are quite remarkable and have provided a basis for their application in promoting growth of blood vessels[77] and nerve regeneration.[78]

4.4. Commensurability and complexity

If one specific type of interaction dominates SA, the structures that form are usually simple. For instance, if square-shaped particles interact both by van der Waals and magnetic dipole–dipole forces (Fig. 10), but the magnitude of the former is much greater than that of the latter, the squares are most likely going to form a closed-packed tiling. On the other hand, if the magnetic forces dominate, the particles are going to line up into chains. The richest variety of phases is expected when the two types of interactions are commensurate so that the vdW forces can bring the particles together while dipole–dipole interactions can introduce directionality into the forming arrays. To generalize, a self-assembling system will exhibit the most structural diversity when the energy is partitioned approximately equally between the interactions acting in the system.

Of course, one should not over-complicate. If the system has too many types of components and/or interactions, the number

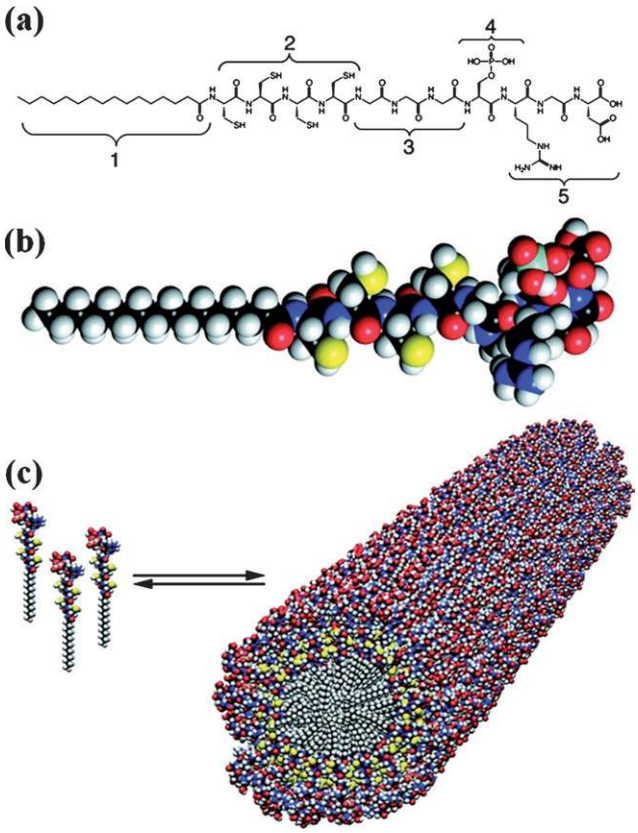

Fig. 9 Stupp's peptide amphiphiles, such as those shown in (a and b) self-assemble into long fibers (c). Reproduced with permission from AAAS, ref. 11.

of possible arrangements having similar free energies can become staggering and one will be faced with the problem of polymorphism discussed at the beginning of Section 4. As an example, consider a system composed of N microspheres self-assembling due to vdW interactions. If all spheres are the same, it does not really matter how the spheres are arranged inside the crystal. If, however, we color half of the spheres red and half blue and expect them to SA into a "chessboard" crystal, we are being somewhat naïve, since the number of ordered arrangements is only $[(N/2)!]^2$ out of the $N!$ possible, and the probability of realizing the perfect chessboard becomes painfully small for large N (specifically, $p \sim e^{-N}$). Of course, for only two particle types, one could bring in additional interactions to help the ordering (*e.g.*, make red spheres positively charged, and the blue

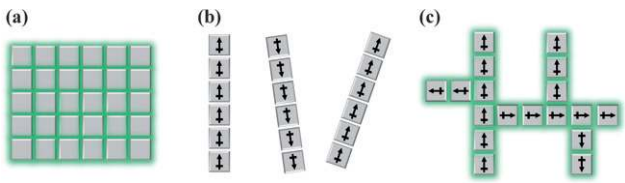

Fig. 10 Commensurability of interaction strengths in SA. (a) Squares interacting *via* vdW attractions form a close-packed tiling. (b) Magnetized squares interact *via* magnetic dipole–dipole forces and form chains. (c) When the strength of the vdW and magnetic forces are commensurate, they "compete" with one another to form more complex structures.

Table 1 Common interactions and their scaling properties useful in designing molecular ESA

Interaction	Range	Scaling relations	References
Ionic (*attractive/repulsive*)	No scale	$\boldsymbol{U} \propto \pm 1/\boldsymbol{r}$ (Coulomb energy). The strength is $\approx$500 kJ mol^{-1} (for two isolated ions at contact)	Ionic crystals[165]
Screened Ionic (*attractive/repulsive*)	1 nm–1μm	$\boldsymbol{U} \propto \pm e^{\kappa r}/\boldsymbol{r}$ where $\kappa^{-1} = (2e^2c_s/k_BT\varepsilon_0\varepsilon)^{-1/2}$is the screening length (k_BT, thermal energy; $\varepsilon_0\varepsilon$, dielectric permittivity of solvent; e, fundamental charge; c_s, salt concentration)	Polyelectrolytes multilayers,[166] global conformation of hammerhead ribozyme[167]
van der Waals (*attractive*)[a]	1 nm–10 nm	$\boldsymbol{U} \propto -1/\boldsymbol{r}^6$ (London dispersion energy). The strength is $\approx$10 kJ mol^{-1} for two alkane molecules (*e.g.*, CH_4, C_6H_6 or C_6H_{12}) in water	Peptide nanofibers,[11] dimeric surfactants[62]
Dipole dipole (*attractive/repulsive*)	0.1 nm–1 nm	$\boldsymbol{U} \propto -1/\boldsymbol{r}^3$ (fixed) and $\boldsymbol{U} \propto -1/\boldsymbol{r}^6$ (rotating, Keesom energy). The strength is $\approx$10 kJ mol^{-1} for two dipoles of strength 1D separated by 0.2 nm	Helical beta-peptides,[168] liquid crystals[169]
Hydrogen-bond (*attractive*)	0.1 nm–1 nm	$\boldsymbol{U} \propto -1/\boldsymbol{r}^2$ (roughly). The strength of most hydrogen-bonds is between 10 and 40 kJ mol^{-1}	Supramolecular architecture,[164] helical chains[170]
Aromatic (π–π) (*attractive*)	0.1 nm–1 nm	Arise from overlapping of p-orbitals in π-conjugated systems. Magnitude scales with the number of π-electrons. Typically the length scale of interaction is $\approx$3.4 Å	Mushroom-shaped architecture,[171] aromatic rods[172]

[a] Repulsive van der Waals interactions are possible only for systems of three materials (molecules of type A can attract a molecule of type B in medium M if the refractive index of the medium, n_M, is between those of the molecules—*e.g.*, $n_A > n_M > n_B$).

ones, negatively charged[16]), but with more particle types, the problem becomes really hard. It is not an accident that the literature on colloidal self-assembly[79,80] has no examples of ternary crystals—they are simply too complex, at least for the time being.

The last comment we add to these heuristic rules is about the types of forces one can use to achieve self-assembly. As you might imagine, the toolbox of self-assembly is quite diverse and virtually any type of physical interaction can be built into a SA system. Some of the most useful types are summarized in Tables 1 and 2 along with scaling relationships which can be used to estimate the magnitudes of these interactions for various sizes of components and/or component separations.

5. Templated and field-directed self-assembly

In addition to the interactions between assembling components, self-assembly may also be facilitated by the use of external templates and fields (*e.g.*, electric, magnetic) which guide the organization of the final structure.

5.1 Templated self-assembly

In templated self-assembly (TSA), a prefabricated "template" orients and directs the assembling components to (i) create structures with better long-range order than their non-templated counterparts, (ii) control the morphology of the resulting

Table 2 Interactions between particles and surfaces for ESA

Interaction	Range	Scaling relations	References
Electrostatic (*attractive/repulsive*)	1 nm–1μm	$\boldsymbol{U} \propto \pm e^{\kappa r}/\boldsymbol{r}$ for charged spheres (κ^{-1} is the screening length)	Binary nanoparticle diamond crystals,[16] electrostatically driven colloidal crystals[80,165]
van der Waals (*attractive*)[a]	1–10 nm	$\boldsymbol{U} \propto -1/\boldsymbol{l}$ for spheres near contact ($\boldsymbol{l}$ is the distance between surfaces)	Nanoparticle superlattices[165,79]
Steric (*repulsive*)	1–100 nm	$\boldsymbol{U} \propto e^{-l/R_g}$ for two surfaces with grafted polymers (R_g is the radius of gyration)	Biospecific binding to mixed SAMs,[173] polystyrene-block-poly(4-vinylpyridine) aggregates in DMF/H_2O[174,165]
Hydrophobic (*attractive*)	1–100 nm	$\boldsymbol{U} \propto -e^{-l/\lambda}$ for two hydrophobic surfaces in water ($\lambda \approx$ 1–2 nm is characteristic length scale)	Hydrophobic gold nanorods,[175] 3D assembly of microscale gold/SiO_2 particles[176,165]
Capillary/menisci (*attractive/repulsive*)	0.1–10 mm	$\boldsymbol{U} \propto \pm\ln(\boldsymbol{r}/L_c)$ for two floating spheres near contact (L_c is the capillary length)	Hexagonal plates on water/perfluorodecalin interface,[177] cheerios effect[178]

[a] Repulsive Van der Waals interactions are possible only for systems of three materials (particles of type A can attract a particle of type B in medium M if the refractive index of the medium, n_M, is between those of the particles—*e.g.*, $n_A > n_M > n_B$).

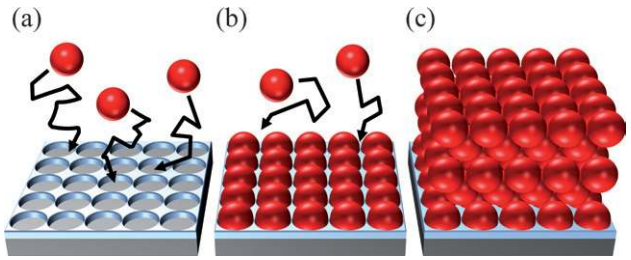

Fig. 11 Templated self-assembly on a surface. (a) Colloidal spheres (*red*) sediment onto a substrate (*grey*) presenting a regular array of microscopic depressions. (*light blue*). (b) After a single monolayer of colloids forms, the colloids remaining in solution must stack on top of this layer in an unambiguous arrangement that ultimately leads to a perfect f. c. c. crystal (c). Scheme is based on the work of van Blaaderen *et al.*, ref. 80.

assemblies, and/or (iii) form novel structures/phases that would be otherwise unfavorable in the absence of the template.

In many forms of templated self-assembly (TSA), the template is composed of a two-dimensional substrate that is chemically or mechanically patterned in order to interact selectively with the assembling components (Fig. 11). In this way, the organization of components near the substrate is governed largely by the pattern on the template, and this order is propagated into the "bulk" of the assembling structure *via* the interactions between the components. For example, when colloidal spheres are crystallized onto a substrate patterned with an array of cylindrical holes, they form a nearly perfect f.c.c. crystal without the stacking faults common to non-templated crystallization (*cf.* Fig. 11).[80] Similarly, both chemically[81,82] and mechanically[83,84] patterned surfaces have been used to template the microphase separation of block copolymers[85] to give long-range ordering of "striped" lamellar phases,[81] one-dimensional arrays of spherical domains,[84] and increasingly complex device-oriented architectures.[82] At the atomic/molecular level, epitaxy has long been the preferred route to monocrystalline films whereby crystal growth is templated by existing crystal planes. This approach can also be extended to chemically patterned surfaces, in which the nucleation density and the crystallographic orientation can be controlled by molecular recognition with the underlying template.[86]

Such interfacial templating is not limited to 2D substrates but can also employ linear, one-dimensional templates—most notably DNA. In addition to its function as a biological template, DNA has been used to template the organization of nanoparticle chains,[87,88] protein arrays,[88,89] as well as nanoscale wires from metals[89,90] and conductive polymers.[91,92] In these examples, the DNA template binds selectively to the components to prearrange the assembly; subsequently, the components can be joined together permanently at which point the template is no longer needed.

Another approach towards TSA is the use of geometric confinement either to orient bulk structures or to induce the formation of novel morphologies not found in bulk systems. The effects of spatial confinement are clearly illustrated in the self-assembly of block copolymer microdomains confined within cylindrical channels[85] (Fig. 12a). Here, the shape and size of the channel determines the orientation and morphology of the microdomains—*e.g.*, lamellar domains wrap to form concentric lamellae when confined to a cylindrical tube.[93–95] When, however, the diameter of the confining channel is incommensurate with the

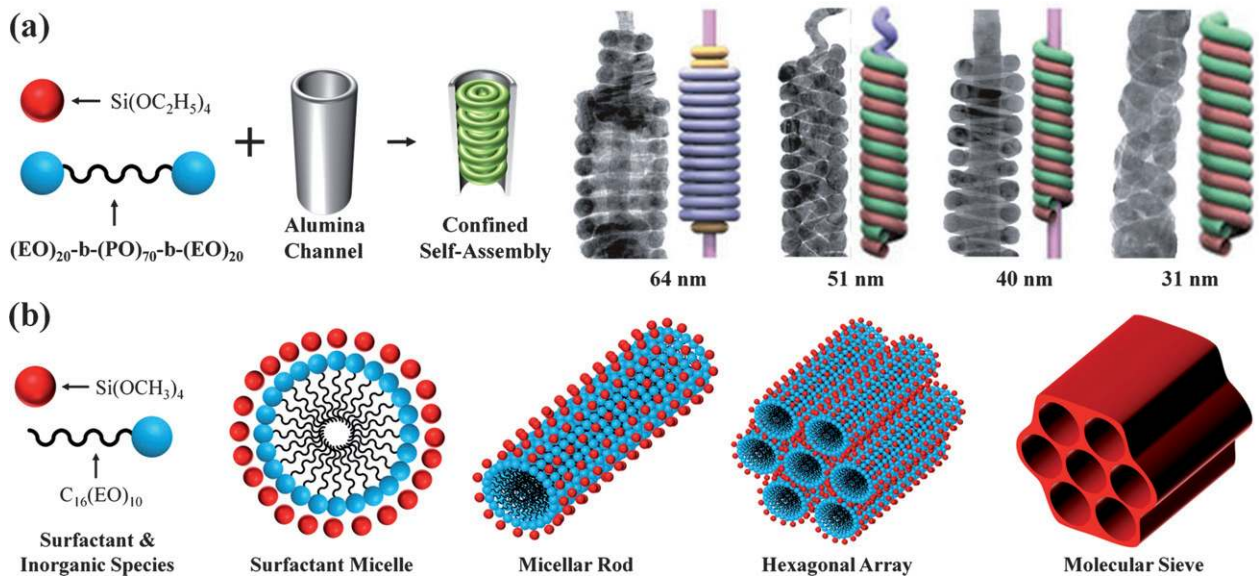

Fig. 12 Confinement based and hierarchical TSA. (a) (left) A triblock copolymer (blue-tail-blue) and tetraethyl orthosilicate (red) confined to narrow channels (grey tube) self-assemble into various copolymer-silica composite structures (green). (right) These structures change with the channel diameter (here, decreasing from 64 nm to 31 nm). The left portion in each pair is a TEM image; the right portion is a scheme of the assembled structure; colors are used only for clarity. Adapted with permission from ref. 97. Copyright 2004 Nature Publishing Group. (b) A scheme of hierarchical TSA. In this example (inspired by the work of Beck *et al.*, ref. 102), a solution of surfactants (*e.g.*, a diblock copolymer, blue sphere with tail) and an inorganic species (tetramethyl orthosilicate, red) self-assemble to form micellar rods, which further assemble into a close-packed hexagonal array of rods. This hexagonal array acts only as a template for the inorganic species that, after heating and calcination, condenses/polymerizes to form the final structure.

natural "period" of the lamellae, the system becomes "frustrated" and adopts more complex toroidal or helical morphologies not observed in bulk systems.[94,96,97] Of course, the effects of confinement on TSA are by no means limited to polymer systems—*e.g.*, colloidal crystallization in liquid droplets can result in unique close-packed clusters[98] as well as larger hemispherical assemblies.[99,100]

Finally, TSA is often used in a hierarchical manner in which a given self-assembled structure is used as a template for higher-order assemblies. This is illustrated by the many forms of surfactant-templated self-assembly, in which surfactants and one or more inorganic compounds organize from solution to form a three-dimensional micellar array that encapsulates the inorganic species within the continuous region between the micelles (Fig. 12b).[101–104] Subsequently, this self-assembled structure provides a template for a porous inorganic material formed by polymerization/condensation of the inorganic species and removal of the sacrificial surfactant template. Similarly, the self-assembled microdomains of block copolymers can subsequently be used in a hierarchical fashion as templates for the assembly of metal nanostructures such as wires and nanoparticle chains.[105]

5.2 Field-directed self-assembly

Like physical templates, externally applied electric, magnetic, and optical fields can also be used to direct the self-assembly process. Field-directed SA has the added advantage that fields can be switched on/off and tuned dynamically. Specifically, when the applied field is static and time independent, it behaves like a physical template, modifying the free energy landscape on which the components evolve and guiding their assembly toward structures characterized by new energy minima. For example, optical fields (*i.e.*, standing electromagnetic waves) can be used to direct polarizable particles to regions of highest field strength (*e.g.*, as in "optical tweezers" comprised of crossed laser beams).[106] In this way, carefully designed optical fields have been used to template three-dimensional colloidal crystals[106] as well as two-dimensional colloidal assemblies used for subsequent epitaxial growth.[107] Similarly, uniform electric fields can be used to template assemblies with improved long-range order and controlled orientation. With diblock copolymers, for example, annealing under an applied electric field results in highly ordered lamellar[108] and cylindrical domains,[109] in which the domain boundaries orient along the field lines. Ordered phases can also be achieved by using applied shear forces.[110] Finally, static magnetic fields are capable of orienting the magnetic domains of magnetic nano- and microparticles, which then self-assemble into well ordered chains *via* dipole–dipole interactions.[111] More complex structures result when the applied field is spatially non-uniform—*e.g.*, large 2D colloidal pyramids assembled under inhomogeneous magnetic fields (*cf.* Fig. 13a and b).[112]

While the above examples of self-assembly under static fields closely resemble those of physical templates, the use of time varying fields can result in assembly strategies with no template-like analogue. In general, the use of time varying fields in self-assembly has two distinct purposes. On one hand, it can be used to agitate (see Section 4.1) an equilibrium structure in order to allow energetically unfavorable defects to be removed from the system. This agitation concept has been successfully applied to

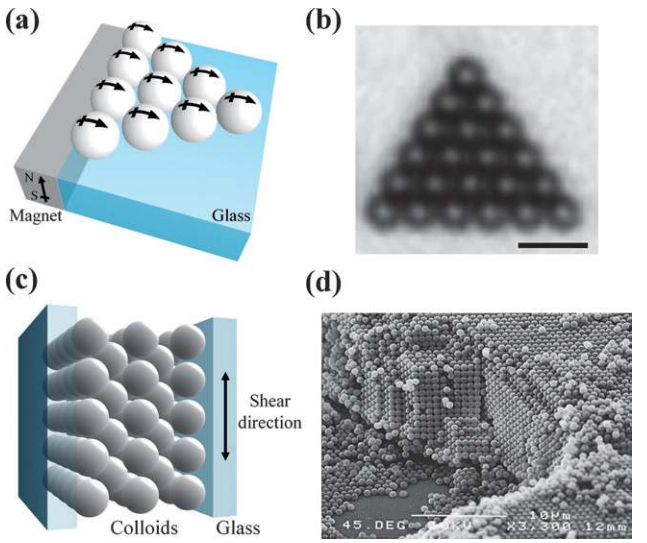

Fig. 13 Static vs. time varying fields in self-assembly. (a) A scheme of a 2D colloidal pyramid assembled in an inhomogenous but static magnetic field; (b) the corresponding experimental realization. Scale bar is 10 μm. Reprinted with permission from ref. 112. Copyright 2005 American Chemical Society. (c) Colloids between two glass plates, shown in this scheme, are agitated into place by oscillating shear forces to form (d) a highly ordered colloidal crystal. Reprinted with permission from ref. 113. Copyright 1997 by the American Physical Society.

the formation of highly ordered colloidal crystals (see Fig. 13b and c) where oscillating shear forces[113] or electric fields[114] act to anneal the particles towards the equilibrium configuration. Alternatively, time varying fields can be used to establish and sustain a dynamically self-assembled system. For example, rotating magnetic fields have been used to assemble dissipative structures comprised of rotating magnetic "spinners" (*cf.* Section 6, Fig. 14)[37,38,115,116] or, more recently, non-magnetic particles immersed in magnetic fluid.[117] The following sections will elaborate on these and other examples as we transition into the exciting world of dynamic self-assembly far from thermodynamic equilibrium.

6. Non-equilibrium/dynamic self-assembly

However intricate, the structures self-assembled at thermodynamic equilibrium are limited by their static nature. This is in contrast to biology, where many of the self-assembled systems can adapt their mode of organization and function in response to external stimuli, self-heal their structures when "wounded," and even self-replicate. To be able to do these things, biological systems escape thermodynamic equilibrium and self-assemble in metastable states dependent on an external supply of energy. Usually, biological DySA involves synchronous action of multiple agents/interactions of which some are designed to bring components together and some to separate them.

Biological DySA occurs on scales from the molecular to the organismal. At the molecular level, the genetic code of life—persistent over eons through replication of DNA, transcription to RNA, and translation into functional proteins—represents a finely tuned symphony of DySA processes. For example, the replication of DNA is energetically driven by the hydrolysis of

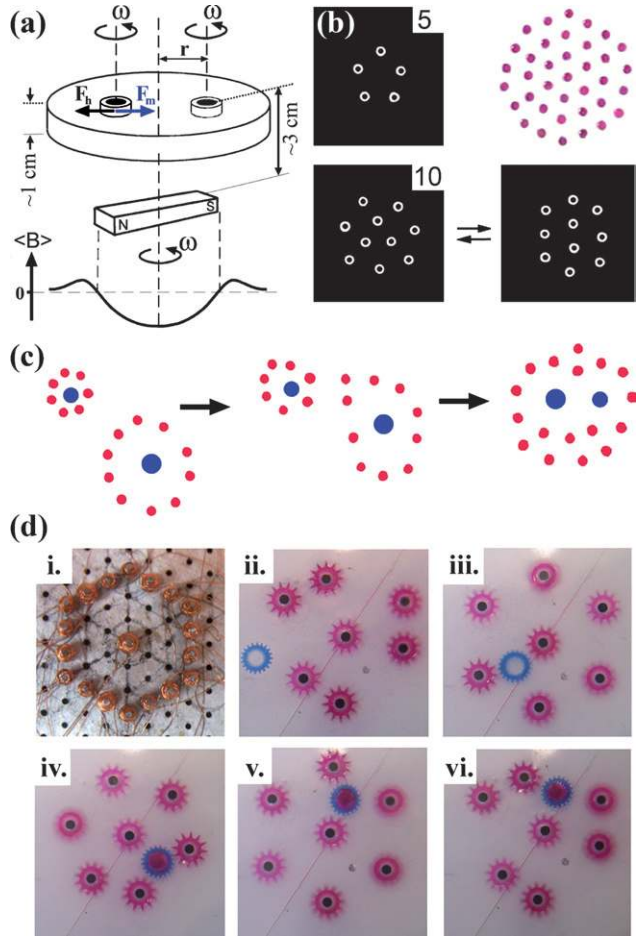

Fig. 14 Magnetohydrodynamic self-assembly. (a) The simplest version of the experimental arrangement used in DySA of magnetic particles. Polymeric discs (0.02–2 mm in diameter) doped with magnetite are placed at a liquid–air interface above a permanent bar magnet rotated with angular velocity ω (200–1100 RPM). The rotating magnet creates an average magnetic force F_m that attracts all discs towards the magnet's axis of rotation. The graph below the scheme has the profile of the average radial component of the magnetic induction—proportional to the energy of the magnetic field—in the plane of the interface. Additionally, the spinning discs repel one another by pairwise hydrodynamic forces F_h. (b) Dynamic patterns formed by 5 (top left), 37 (top right), and 10 (bottom) disks. Assemblies of 10 disks can be toggled between two different arrangements. (c) Fusion of two macroscopic "artificial atoms" into an "artificial molecule". The smaller "atom" is composed of one disk 2.08 mm in diameter, and seven disks 1.27 mm in diameter; the larger atom has one 2.42 mm disk and ten 1.27 mm disks. The "atoms" are initially prepared in two separate energy minima created by field concentrators above the plane of the interface, and are "reacted" by moving the concentrators towards each other. (d) A self-assembling fluidic machine that uses seven gears, organized above "activated" electromagnets, to manipulate a non-magnetic container floating at the interface. The carousel first incorporates an empty container (ii), turns it around (iii) until the filling point (iv), completes the revolution (v), expels the filled container (vi), and finally returns to its initial state. The motions of the carrousel are caused by the synchronous activation of the electromagnets. Reprinted with permission from (a) ref. 20 (b) ref. 37, Copyright 2000 Nature Publishing Group, (c) ref. 148, Copyright 2001 American Chemical Society, (d) ref. 19, Copyright 2004 American Institute of Physics.

deoxyribonucleotide triphosphate precursors[118] and entails self-assembly of proteins called helicase, DNA polymerase, and primase proteins. Helicase physically separates the antiparallel strands at the origin of replication,[119] DNA polymerase powered by nucleoside triphosphates synthesizes new Watson–Crick base pairs,[119,120] and ligase seals the new strands together[121] before returning the system to the final equilibrium state.

On the cellular scale, dynamic self-assembly underlies the functioning of the maze of cytoskeletal fibers (microtubules and actin filaments), which are responsible for the cell's structural integrity, mechanical resilience, and ability to move.[122,123] The unique features of these self-assembling polymers are that they are maintained in a state of non-equilibrium balance between assembly at one end and disassembly on the other, and that the assembly steps require a constant supply of chemical energy (in the form of GTP or ATP) to prevent the fibers from so-called "catastrophing" and ultimately shrinking.[124,125]

Finally, on the scale of cellular or bacterial populations, DySA mediates collective behaviors including the formation of spatial patterns as wells as swarming (see the review by Weibel *et al.* in this issue). For instance, in bacterial colonies, communication mediated by chemicals each member secretes into the surrounding medium allows the group to adjust to changing nutrient conditions. When nutrients are abundant, bacteria form circular aggregates; when food (that is, energy!) is scarce, they organize into fractal or vortex-like structures to maximize the efficiency of food consumption.[126,127] The underlying assembly mechanism relies on the coupling of the local reproduction rate to the diffusive delivery and consumption of nutrients.[127]

The take-home message from these examples is quite simple: DySA is much more powerful than equilibrium SA, and it is only through this mode of SA that we can ever dream of self-assembling "intelligent" materials that can adapt, self-propel, or self-replicate. For all of these behaviors, a system must be able to alter its internal organization, and it can do so only if its free energy "status" can change. This is synonymous with being non-equilibrium.

7. Theory of DySA—still in the making

Unfortunately, the theory of DySA cannot be created by a simple extension of equilibrium thermodynamics, for in non-equilibrium states, the familiar thermodynamic potentials lose their meaning. In fact, despite decades of research,[41,128–132] there is no coherent theory of non-equilibrium systems, though there are some exciting insights and developments.

In terms of fundamental thermodynamic characteristics, DySA structures belong to a broad class of non-equilibrium (NE) steady-state systems. Importantly, since the fundamental law of entropy maximization is not valid in the non-equilibrium regime, DySA systems can "reside" in low entropy states and are able to organize themselves into complex spatial or coherent spatio-temporal structures,[41,128,129] which can be maintained only by dissipating energy into the environment and thus increasing its entropy.

For NE systems close to equilibrium, Nicolis and Prigogine[128] proposed their famous variational principle called the minimal entropy production (MEP) rule. If the change, dS, of the

system's total entropy is written as a sum of entropy produced in this system by irreversible processes, dS_P, and the entropy flow due to exchange of energy or work between the system and its environment, dS_f, then the MEP rule stipulates that the rate of entropy production, $P = dS_P/dt$, is minimal at steady-state (and, of course, $dS = 0$ therein). While this law has proven remarkably useful in many cases,[128,129] it must be remembered that it applies only to "linear non-equilibrium thermodynamics," where the Onsager's reciprocal relations[129] hold, and the assumption of local thermodynamic equilibrium is valid. Unfortunately, in the linear regime, the system is uniform and dissipative structures are not observed.[128] They appear only far from equilibrium, when the "linear" steady-state becomes unstable, and the system "switches" to an ordered configuration *via* a bifurcation mechanism[128,129] induced by changes in external forces/parameters (*e.g.*, the frequency of the rotating magnetic field in the case of self-assembling spinners; *cf.* Section 9.1).

Recognizing the limitation of these theories, several groups have recently attacked the problem starting at the microscopic level and using both numerical[133–136] and analytical tools of statistical mechanics.[137–140] This work has lead to some exciting developments—notably, the Jarzynski equality,[141,142] which relates free energy differences between two equilibrium states *via* ensemble averages over non-equilibrium pathways connecting them, and the Crooks relation,[143,144] which generalizes Jarzynski's non-equilibrium work relation and connects to the fluctuation theorems. Another promising approach has been the study of the phase space of NE systems.[130,132] Within this approach, the second law of thermodynamics governing the system's evolution can be related to the geometry and topology of the phase space. Specifically, as a NE system described by deterministic equations of motion evolves, its phase space probability distribution function, $f(\boldsymbol{\Gamma}(t),t)$, collapses ("shrinks"). For a system of N particles, $f(\boldsymbol{\Gamma}(t),t)$ is a function of the space vector, $\boldsymbol{\Gamma}(t) = (\boldsymbol{q}_1(t),\ldots, \boldsymbol{q}_N(t); \boldsymbol{p}_1(t),\ldots, \boldsymbol{p}_N(t))$, where $\boldsymbol{q}_i(t)$ and $\boldsymbol{p}_i(t)$ stand, respectively, for the position and momentum of the ith particle. Eventually, the system reaches its non-equilibrium steady-state with phase space characterized by a complicated set of fractal structures called a strange attractor[130,145] (Fig. 2b). Phase space compression is related to the loss of the system's dimensionality,[130,132,135] and is facilitated by a continuous flow of entropy, which is transferred from the system to its surroundings. In other words, as the system organizes itself, the phase space available to its components becomes smaller; the larger the change in the degree of system's ordering (per unit time), the more entropy is produced and transferred to the environment.

Finally, attempts have been made to relate the forces acting between the components of a DySA system to the rate of entropy production at the system's steady-states. A paper by Tretiakov *et al.* later in this issue explains this approach in more detail and demonstrates its usefulness to systems, in which Prigogine's MEP production fails.

More thorough discussion of these and other theoretical concepts can also be found in our recent review on DySA.[146]

8. Design of DySA systems

As in the case of equilibrium SA, the design of non-equilibrium SA systems can be guided by a set of common-sense rules which we have described in detail in ref. 146 and 147 and here review only briefly:

8.1. Identifying suitable interactions

The first necessary condition for DySA is that at least one type of interaction acting in the system must depend on and be regulated by externally delivered energy (if the changes in energy supply have no effect on the system's components, the system would be energetically isolated and not a dissipative one). Table 3 gives some examples of forces that can be coupled to external sources of energy in the form of various fields.

8.2. Choosing "competing" interactions

Similar to some of the heuristics of equilibrium SA, a DySA system should incorporate interactions that "compete" with one another. If the only forces acting between the components are repulsive, the system will simply fall apart; if they are all attractive, the system might dynamically aggregate, but the aggregate will not develop order beyond, at best, simple close packing. Only by having "competing" attractions and repulsions is it possible to introduce selectivity into the system.

8.3. Choosing a proper length scale

To build a steady-state dynamic structure, a proper environment and length scale must be chosen such that the opposing (attractive-repulsive) forces are similar in magnitude and can therefore balance one another. The choice of these system parameters comes from knowledge of how the individual interactions scale with object size, distance from other objects, and with the material properties of the surrounding medium. Specific scaling laws can be found in ref. 146.

8.4. Synthesis

This rule is somewhat subjective and is based on the experience of our laboratory. Since DySA is usually a complicated process, dynamically self-assembling systems should be built from simple components; only after the simplest system is built and understood in quantitative detail, should one "complexify" by adding new types of components/interactions. Conceptually, this approach is akin to synthetic methods of chemistry, where one progresses "bottom-up" from simple reactants to complex products. We advocate this methodology over the recent trend in systems' science which focuses on the analysis of inherently complex assemblies/structures "top-down". The synthetic approach offers better fundamental understanding of and ability to rationally design various levels and aspects of dynamic self-assembly. The next section will illustrate this methodology in practice.

9. Examples of synthetic DySA systems

Here are three systems in which DySA has been engineered using different types of forces at different length scales.

Table 3 Examples of "dynamic forces" for DySA

Interaction	Induced/Addressed by	Particle size/type	Applications and references
Induced magnetic dipole–dipole[179]	Induced by external magnetic field	Ferromagnetic colloids, 0.1–100 μm	SA microfluidic mixers;[20] applications of magnetorheological fluids: automotive clutches,[180] polishing fluids,[181] smart knee prosthetics,[182] anti-lock brakes,[183] vibration control of washing machines;[184] 2D and 3D arrays of electro-magnetorheological colloids,[185,186] active seismic control of buildings[187–192]
Optical binding	Intense optical fields induce long-range forces between dielectric particles	Dielectric colloids 0.1–100 μm	Formation of ordered 2D crystalline arrays of colloidal particles which are held together by light[106,193]
Optical dipole–dipole	Light isomerizes surface bound molecules and induces surface dipoles	Nanoparticles, 5–20 nm	Formation of metastable, 3D nanoparticle supracrystals[157]
2D vortex-vortex	Hydrodynamic flows induced by objects rotating in a fluid create a repulsive force perpendicular to the axis of rotation	μm–mm objects	DySA of magnetized disks at a liquid-air interface;[37,38,115,116,148] self-assembled gear systems and fluidic machines;[19,194] cell membranes with SA arrays of rotating bio-motors;[195] vortex crystals in magnetized electron columns[196,197]
Flow-induced viscous interaction	Induced by viscous coupling between nearby objects translating in a fluid	μm–mm objects	Flow-induced structures in sheared colloidal suspensions[198]
3D vortex columns	Objects rotating above/below one another at two fluid-fluid interfaces experience a repulsive force at low and an attractive force at high angular velocities	μm–mm objects	DySA of 3D vortex crystals[149,199]
Dynamic capillary	Gradients in temperature or the concentration of surface-active agents create non-homogeneous surface tension profiles on a fluid-fluid interface—Marangoni effect. Repulsive interparticle forces are created when the particles, themselves, generate such gradients at an interface, on which they are free to move	μm–mm	Dynamic self-assembly of camphor-doped polymeric particles at the fluid-air interface;[150] dynamic behavior of camphor particles at the fluid-air interface: spontaneous movement,[151] oscillations and symmetry-breaking,[200] mode selection,[201] synchronization of two camphor boats,[202] formation of ordered boat arrays[150]
Induced electric dipole–dipole[203]	DC and AC voltages up to 100 kHz	0.1–100 μm semiconductor particles	Applications of electrorheological fluids: ordered arrays of colloidal particles;[204] smart inks;[205–207] mechanical polishing;[208,209] tactile displays;[210] actuators;[211] dynamic self-assembly in electrostatically driven granular media: crystals, rotating vortices, and pulsating rings[212,213]
Scattered light	Near-infrared light scattering by lysosome-rich cells	~10 μm cells	$3T3_x$ cell aggregation: lysosome-rich cells attract others by their enhanced ability to scatter near-IR light. The cells "feel" each other at distances as large as 200 μm[214]
Light-switch aggregation of magnetic colloids	Recently observed effect—the origin of the interactions is not well understood[215,216]	10 nm magnetic nanoparticles	Fundamental understanding of nanoparticle interactions

9.1. Vortex-vortex DySA

Developed by Grzybowski, Stone, and Whitesides,[37] this system is a classic demonstration on DySA that can be "synthetically" complexified from simple particle assemblies all the way to fluidic machines[19] and micromixers[20] (Fig. 14). In its simplest variation (Fig. 14a), the system consists of a collection of small (tens of microns to millimetres) magnetically-doped particles (usually polymeric disks containing magnetite powder) floating at a liquid-air interface and subject to a field produced by a permanent magnet rotating below this interface. Under the influence of the rotating magnetic field, all disks experience a centrosymmetric (*i.e.*, all-attractive) force, F_m, directed towards the axis of the magnet's rotation. At the same time, their induced magnetic moments interact with the magnetic moment of the external magnet, and the disks rotate around their axes at an angular velocity ω equal to that of the magnet. The fluid motion associated with spinning results in repulsive hydrodynamic

interactions F_h between the disks (*cf.* Fig. 14a). These repulsions[37,115] are dynamic in the sense that they exist only as long as the energy is delivered to the spinners from the external, rotating magnetic field.

Because the magnitudes of attractive magnetic and repulsive hydrodynamic forces are commensurate, the collections of randomly distributed spinners evolve into dynamic open-lattice assemblies capable of a variety of adaptive behaviors (*cf.* Fig. 14b). Since the magnitude of the vortex-vortex repulsions increases with ω, one can control the assembly by tuning the rate of energy supplied to the system. This control parameter enables one to modify the interparticle spacing, effectively expanding or contracting the lattice, or even to toggle the system between different stable configurations or "modes" of assembly (Fig. 14b). In addition to this primitive adaptability, the system is capable of rebuilding itself when perturbed, provided that energy is continuously supplied by the rotating magnetic field. Characteristic of DySA, the assembly "dies" when the flow of energy ceases, and the disks collapse into a disordered cluster.

Building on this basic arrangement, more complex systems were constructed using differently shaped particles or mixtures of component types, leading to assemblies that exhibit stereoselectivity[38] or quantitatively mimic the so-called classical artificial atoms[116] "reacting" with one another to form larger "molecules" (Fig. 14c).[148] Extension of this system to two parallel fluidic interfaces and the introduction of new types of forces acting between spinners at different interfaces was shown to lead to even more complex behaviors including self-replication of patterns.[149]

The most rewarding part of the story is probably the fact that magnetohydrodynamic DySA is not only a laboratory demo, but has been developed to the level of certain practicality. One example is microfluidic mixers[20] where magnetic particles organize and rotate in a microfluidic chamber to mix two laminarly flowing streams. The other example is shown in Fig. 14d where magnetic spinners perform DySA to power simple mechanical "machines" operating at fluidic interfaces.[19] This system consists of two-component rotors, with a magnetic core and a non-magnetic gear-shaped ring around it. When an external rotating magnetic field is applied, the cores begin to rotate and center inside the gears, generating a hydrodynamic flow that sets the gears into motion. Rotors can be manipulated at the interface by localized magnetic fields generated by electromagnetic actuators placed below the liquid's surface. Importantly, because of vortex-vortex repulsions between any two rotors, only one rotor resides in one local energetic minimum, and for a given "pattern" of magnetic field the rotors self-assemble into a unique structure. In other words, configuration and function of these fluidic machines are directed by the self-assembly "template" of magnetic field concentrators. Fig. 14d demonstrates how the rotors can act as a carousel system to move floating containers, fill them with analyte solutions, and deliver them to a specific end location.

9.2. DySA *via* dynamic surface tension

Inspired by chemotactic bacteria that move in response to chemical gradients which they create, our group ventured to create a DySA system in which the components would dynamically self-assemble as a result of chemical "communication" through the chemicals they emit (Fig. 15). Scrutinizing Table 3, we see that dynamic capillary effects are the only type of interaction listed that is related to chemical emission (here, onto a fluid interface). In the specific system we designed,[150] we used collections of the well known camphor boats, which are small hydrogel particles that slowly release a surface-active agent (*e.g.*, solid camphor) onto the interface on which they are placed. As the camphor diffuses from the particles, it creates dynamic gradients in the surface tension, which cause the particles to move about autonomously, further modifying the interface. Importantly, the camphor is removed from the interface *via* sublimation/dissolution into the surrounding environment, thereby maintaining the non-equilibrium conditions.

While the behavior of isolated camphor particles is relatively well understood,[151,152] far more interesting dynamics arise when multiple particles begin to interact dynamically at an interface. At low densities (< 0.3 particles/cm^2; Fig. 15b, left), particles continue to move about autonomously but influence each other through a repulsive, surface-tension-driven interaction, which can be approximated by a pairwise potential. This recently reported interaction[150] can be understood by considering the particles' "desire" to move toward regions of higher surface tension (*i.e.*, lower camphor concentration). When two particles approach one another, the camphor concentration is highest in

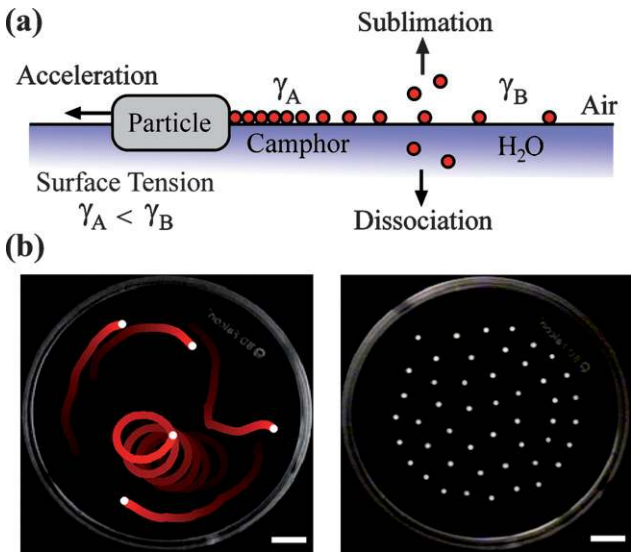

Fig. 15 DySA by dynamic surface tension gradients. Here, hydrogel particles (1 mm in diameter) doped with camphor and floating at a water-air interface move about autonomously and ultimately organize into DySA structures.[150] (a) As camphor diffuses out from the particles and onto the interface, it creates surface tension gradients which result in Marangoni flows within the fluid. These flows cause the particles to move on the interfaces and lead to repulsive hydrodynamic interactions between particles. Because camphor is steadily removed from the interface *via* sublimation into the gas phase and dissociation into the fluid phase, the system is always maintained in its dynamic, non-equilibrium state. (b) For low particle densities (left), the particles move about autonomously, interacting with one another *via* repulsive hydrodynamic interactions. At sufficiently high densities (right), the particles organize into an open lattice due to these repulsive interactions and geometric confinement. (b) (right) Reproduced with permission from ref. 150. Copyright 2008 American Chemical Society. Scale bars = 5 mm.

between the particles, creating a region of low surface tension from which the particles are "pulled" by surrounding areas of higher surface tension.

At higher densities, however, particles slow down as the interface becomes saturated with camphor and ultimately evolve into steady DySA structures (Fig 15b, right). These steady, non-equilibrium formations are characterized by roughly hexagonal packing in which repulsive interactions are balanced by geometric confinement; qualitatively similar patterns are observed in bacterial colonies that organize to optimize food consumption. Like all DySA systems, the resulting structures are stable against small fluctuations and respond/adapt to perturbations in the environment (*e.g.*, a change in the shape of the interface).

9.3. Nanoscale DySA *via* photoinduced dipole–dipole forces

Macroscopic systems always leave something to be desired—their very scale. To chemists, at least, anything larger than a few ångströms or nanometres is usually a toy system (probably, rightfully so). Can DySA be miniaturized to such small scales? In this context, an inherent advantage of being small is that thermal noise is appreciable and can serve as the "repulsive" interaction to break up the assembling structures. Consequently, one only needs to engineer a dynamic attractive force of comparable magnitude into a system to meet the DySA design criteria 7.1–7.3. One way of doing so is through surface modification of the components with molecules whose properties (*e.g.*, charge, dipole moment, etc.) can be switched "on-demand" by an external stimulus. The functionalization schemes are particularly straightforward with metal and semiconductor nanoparticles and are usually based on self-assembled monolayers.[8,10] There are also many types of switchable molecules such as rotaxanes,[153–155] spiropyranes, or azobenzenes.[156] The azobenzenes are particularly convenient to use since (i) they are easy to synthesize; (ii) their *trans-cis* photoisomerization with UV light induces large dipole moments (on the order of several Debye); (iii) since in the absence of UV irradiation, the molecules reisomerize to the no-dipole *trans* form, the presence of dipolar interactions is dependent upon a continuous flux of energy (Fig. 16).

Based on these premises, we synthesized noble metal nanoparticles (NPs) covered with mixed SAMs containing a fraction of azobenzene containing alkane thiols (ATs). The proportion of the ATs in the monolayer was adjusted such that the interactions between light-induced dipoles on different nanoparticles were commensurate with (see rule 7.3) and slightly stronger than the magnitude of thermal noise ($3/2k_BT$), which tends to disrupt any NP–NP assemblies.

The DySA system thus constructed[157] behaved exactly as planned. Upon UV irradiation, the NPs formed large, three-dimensional supracrystals such as those shown in Fig. 16b. These crystals were metastable and when UV was turned off, they spontaneously fell apart due to thermal agitation. The cycle was fully reversible for at least several hundred cycles, and the metastable state was always well ordered. All in all, this system demonstrates the feasibility of DySA engineering at the nanoscale and in three dimensions. Similar designs can no doubt be extended to other types of NPs and assembled structures.

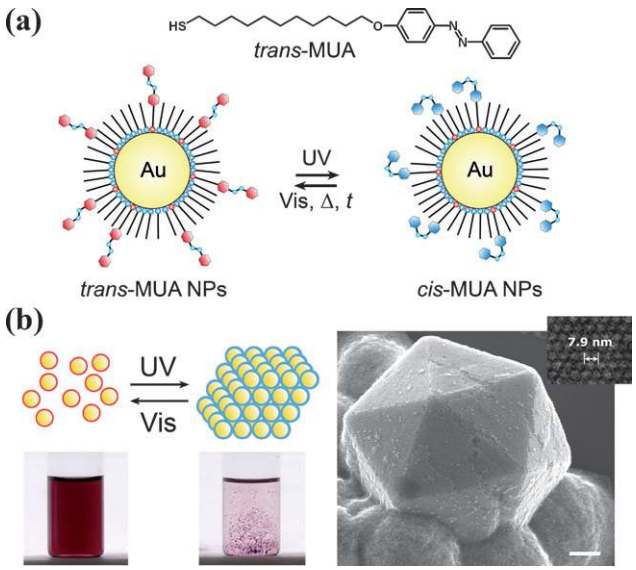

Fig. 16 (a) Structure of *trans*-4-(11-mercaptoundecanoxy)azobenzene (MUA, *top*). UV irradiation of nanoparticles (here, gold) covered with a mixed monolayer of MUA and dodecylamine (DDA) causes photoisomerization of *trans*-MUA to the *cis* form. The *cis* isomer reverts to the *trans* form either spontaneously (slowly), or upon irradiation with visible light, or by heating (both, rapidly). (b) Dipole–dipole interactions between *cis*-MUA molecules ($\mu \approx 4$ Debye) decorating the NPs surface cause the particles to organize reversibly into metastable crystals which persist only under continuous UV irradiation. Visible irradiation results in the *cis*-to-*trans* reisomerization of MUA and the dissolution of the NP crystals.[157] Scale bar = 200 nm. Reproduced with permission from ref. 157. Copyright 2007 by the National Academy of Sciences of the United States of America.

9.4. What do we learn?

The lesson from these examples is that although DySA is still in its infancy, it can be rationally designed from various interactions and at different length scales. The ability to engineer ordered, non-equilibrium states opens some exciting possibilities for conceptually new types of materials that can be reconfigured on-demand. These systems can be useful in several contexts: they can become sensors and chemical amplifiers responding to environmental stimuli by changing their mode of organization; they can conceivably become adaptive (if feedback loops are built in); and they can even be useful for energy storage, since metastable states can be high in energy they can later liberate. We do think that non-equilibrium is the future of self-assembly—especially if we are serious about using SA as skilfully as the inherently non-equilibrium living systems do.

10. The outlook: bioinspired DySA and the junction with self-organization

In this closing section, we will allow ourselves to be bioinspired and speculate about the SA systems of the future, at least the way we see it. In the Review, we focused on external fields (electromagnetic, magnetic, etc.) that provide energy inputs for the specific interactions mediating DySA. In biology, this mode of non-equilibrium delivery is important (*e.g.*, in photosynthesis), but it is not the predominant one. Most of the time, biological

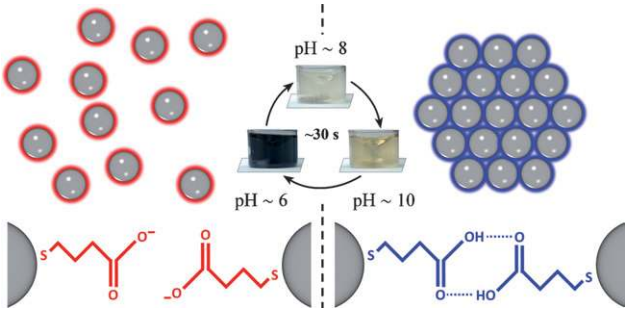

Fig. 17 A vision for pH-driven self-assembly coupled to a chemical oscillator. Here, the oscillator cycles the pH of the solution between 6 and 10, which in turn causes the molecules on the particles' surfaces to protonate/deprotonate and self-assemble/disassemble as their attractive interactions are turned on and off.

systems maintain their non-equilibrium status by chemical means, using complex biochemical networks displaced from equilibrium. Such displacement can be achieved by coupling chemical reactions with transport phenomena such as diffusion (or convection, or active transport). Reaction-diffusion systems[158,159] are inherently non-equilibrium and can set up chemical gradients that then provide time varying fluxes of chemicals necessary to power DySA. In the context of DySA design, it is important to note that chemical networks[160,161]—unlike the relatively few "dynamic" interactions listed in Table 3—are virtually unlimited in their structure, types of participating chemicals, and/or feedback/autocatalytic loops. In other words, out-of-equilibrium reaction networks can provide very versatile controls for dynamic self-assembly. Here lies a great opportunity for the junction of DySA and self-organizing chemical systems that use chemical reaction networks and transport processes to achieve various types of oscillatory or wave-generating behaviors. The biggest challenge is to couple these networks with DySA. A notable step in this direction is the recent work of Epstein and co-workers[162] who demonstrated the coupling of a chemical oscillator with the precipitation/dissolution process. What is needed is more such systems and ones that would be able to achieve ordered/functional states. One possible example of coupling a chemical clock to DySA is illustrated in Fig. 17 and is based on work our group currently pursues. The big hope is that by starting with even relatively simple reaction networks and self-assembly phenomena, we will be able to gradually develop these systems and engineer non-equilibrium DySA states of complexity approaching that of biological systems. So, all hands on deck—there is plenty of work to do!

References

1 G. R. Desiraju, *Angew. Chem. Int. Ed.*, 1995, **34**, 2311–2327.
2 B. Moulton and M. J. Zaworotko, *Chem. Rev.*, 2001, **101**, 1629–1658.
3 J. Aizenberg, D. A. Muller, J. L. Grazul and D. R. Hamann, *Science*, 2003, **299**, 1205–1208.
4 A. J. Blake, N. R. Champness, P. Hubberstey, W. S. Li, M. A. Withersby and M. Schroder, *Coord. Chem. Rev.*, 1999, **183**, 117–138.
5 J. M. Lehn, *Angew. Chem. Int. Ed.*, 1990, **29**, 1304–1319.
6 D. Philp and J. F. Stoddart, *Angew. Chem. Int. Ed.*, 1996, **35**, 1155–1196.
7 D. Whang, S. Jin, Y. Wu and C. M. Lieber, *Nano Lett.*, 2003, **3**, 1255–1259.
8 J. C. Love, L. A. Estroff, J. K. Kriebel, R. G. Nuzzo and G. M. Whitesides, *Chem. Rev.*, 2005, **105**, 1103–1169.
9 C. D. Bain, E. B. Troughton, Y. T. Tao, J. Evall, G. M. Whitesides and R. G. Nuzzo, *J. Am. Chem. Soc.*, 1989, **111**, 321–335.
10 D. Witt, R. Klajn, P. Barski and B. A. Grzybowski, *Curr. Org. Chem.*, 2004, **8**, 1763–1797.
11 J. D. Hartgerink, E. Beniash and S. I. Stupp, *Science*, 2001, **294**, 1684–1688.
12 J. D. Hartgerink, E. Beniash and S. I. Stupp, *Proc. Natl. Acad. Sci. USA*, 2002, **99**, 5133–5138.
13 C. A. Mirkin, R. L. Letsinger, R. C. Mucic and J. J. Storhoff, *Nature*, 1996, **382**, 607–609.
14 M. Li, H. Schnablegger and S. Mann, *Nature*, 1999, **402**, 393–395.
15 S. J. Park, A. A. Lazarides, C. A. Mirkin and R. L. Letsinger, *Angew. Chem. Int. Ed.*, 2001, **40**, 2909–2912.
16 A. M. Kalsin, M. Fialkowski, M. Paszewski, S. K. Smoukov, K. J. M. Bishop and B. A. Grzybowski, *Science*, 2006, **312**, 420–424.
17 S. S. Fan, M. G. Chapline, N. R. Franklin, T. W. Tombler, A. M. Cassell and H. J. Dai, *Science*, 1999, **283**, 512–514.
18 M. Yan, H. T. Zhang, E. J. Widjaja and R. P. H. Chang, *J. Appl. Phys.*, 2003, **94**, 5240–5246.
19 B. A. Grzybowski, M. Radkowski, C. J. Campbell, J. N. Lee and G. M. Whitesides, *Appl. Phys. Lett.*, 2004, **84**, 1798–1800.
20 C. J. Campbell and B. A. Grzybowski, *Philos. Trans. R. Soc. Lond. Ser. A*, 2004, **362**, 1069–1086.
21 M. Fialkowski, A. Bitner and B. A. Grzybowski, *Nat. Mater.*, 2005, **4**, 93–97.
22 Z. D. Cheng, W. B. Russell and P. M. Chaikin, *Nature*, 1999, **401**, 893–895.
23 A. D. Dinsmore, M. F. Hsu, M. G. Nikolaides, M. Marquez, A. R. Bausch and D. A. Weitz, *Science*, 2002, **298**, 1006–1009.
24 T. D. Clark, J. Tien, D. C. Duffy, K. E. Paul and G. M. Whitesides, *J. Am. Chem. Soc.*, 2001, **123**, 7677–7682.
25 T. D. Clark, R. Ferrigno, J. Tien, K. E. Paul and G. M. Whitesides, *J. Am. Chem. Soc.*, 2002, **124**, 5419–5426.
26 D. H. Gracias, J. Tien, T. L. Breen, C. Hsu and G. M. Whitesides, *Science*, 2000, **289**, 1170–1172.
27 M. Boncheva, S. A. Andreev, L. Mahadevan, A. Winkleman, D. R. Reichman, M. G. Prentiss, S. Whitesides and G. M. Whitesides, *Proc. Natl. Acad. Sci. USA*, 2005, **102**, 3924–3929.
28 B. A. Grzybowski, A. Winkleman, J. A. Wiles, Y. Brumer and G. M. Whitesides, *Nat. Mater.*, 2003, **2**, 241–245.
29 A. Winkleman, B. D. Gates, L. S. McCarty and G. M. Whitesides, *Adv. Mater.*, 2005, **17**, 1507–1511.
30 H. J. J. Yeh and J. S. Smith, *IEEE Phot. Tech. Lett.*, 1994, **6**, 706–708.
31 Alien Technology website: http://www.alientechnology.com/products/fsa/.
32 M. J. Heller, J. M. Cable and S. C. Esener, Methods for electronic assembly and fabrication of devices, U.S. Patent 6 652 808, 2003.
33 IBM Website: http://www-03.ibm.com/press/us/en/pressrelease/21473.wss.
34 D. G. Grier, *Nature*, 2003, **424**, 810–816.
35 K. E. Strecker, G. B. Partridge, A. G. Truscott and R. G. Hulet, *Nature*, 2002, **417**, 150–153.
36 B. A. Grzybowski, J. A. Wiles and G. M. Whitesides, *Phys. Rev. Lett.*, 2003, **90**, 083903.
37 B. A. Grzybowski, H. A. Stone and G. M. Whitesides, *Nature*, 2000, **405**, 1033–1036.
38 B. A. Grzybowski and G. M. Whitesides, *Science*, 2002, **296**, 718–721.
39 J. W. Hill and R. H. Petrucci, *General Chemistry: An Integrated Approach*, Prentice Hall, Upper Saddle River, NJ, 2002.
40 P. Meakin, P. Ramanlal, L. M. Sander and R. C. Ball, *Phys. Rev. A*, 1986, **34**, 5091–5103.
41 M. C. Cross and P. C. Hohenberg, *Rev. Mod. Phys.*, 1993, **65**, 851–1112.
42 A. V. Getling, *Rayleigh-Benard Convection: Structures and Dynamics*, World Scientific, River Edge, NJ, 1998.
43 R. J. Field and M. Burger, *Oscillations and Traveling Waves in Chemical Systems*, John Wiley & Sons, New York, 1985.
44 J. Ross, S. C. Muller and C. Vidal, *Science*, 1988, **240**, 460–465.
45 I. Epstein and J. A. Pojman, *An Introduction to Nonlinear Chemical Dynamics: Oscillations, Waves, Patterns, and Chaos*, Oxford University Press, New York, 1998.

46 A. M. Turing, *Philos. Trans. R. Soc. London, Ser. B*, 1952, **237**, 37–72.
47 I. Lengyel, S. Kadar and I. Epstein, *Science*, 1993, **259**, 493–495.
48 H. A. Klok and S. Lecommandoux, *Adv. Mater.*, 2001, **13**, 1217–1229.
49 C. Park, J. Yoon and E. L. Thomas, *Polymer*, 2003, **44**, 6725–6760.
50 B. J. Holliday and C. A. Mirkin, *Angew. Chem. Int. Ed.*, 2001, **40**, 2022–2043.
51 N. Bowden, I. S. Choi, B. A. Grzybowski and G. M. Whitesides, *J. Am. Chem.Soc.*, 1999, **121**, 5373–5391.
52 B. A. Grzybowski, N. Bowden, F. Arias, H. Yang and G. M. Whitesides, *J. Phys. Chem. B*, 2001, **105**, 404–412.
53 B. A. Grzybowski, M. Fialkowski and J. A. Wiles, *J. Phys. Chem. B*, 2005, **109**, 20511–20515.
54 J. A. Wiles, B. A. Grzybowski, A. Winkleman and G. M. Whitesides, *Anal. Chem.*, 2003, **75**, 4859–4867.
55 J. Lowell and A. C. Roseinnes, *Adv. Phys.*, 1980, **29**, 947–1023.
56 M. Adams, Z. Dogic, S. L. Keller and S. Fraden, *Nature*, 1998, **393**, 349–352.
57 S. Fraden, G. Maret, D. L. D. Caspar and R. B. Meyer, *Phys. Rev. Lett.*, 1989, **63**, 2068–2071.
58 L. Onsager, *Ann. NY Acad. Sci.*, 1949, **51**, 627–659.
59 K. R. Purdy and S. Fraden, *Phys. Rev. E*, 2004, **70**, 8.
60 G. Bai, J. Wang, H. Yan, Z. Li and R. K. Thomas, *J. Phys. Chem. B*, 2001, **105**, 3105–3108.
61 C. Tanford, *The Hydrophobic Effect*, Wiley-Interscience, New York, 1980.
62 G. Bai, Y. Wang, H. Yan and R. K. Thomas, *J. Colloid Interface Sci.*, 2001, **240**, 375–377.
63 S. A. Chen, H. M. Xi and L. Yu, *J. Am. Chem. Soc.*, 2005, **127**, 17439–17444.
64 S. R. Batten and R. Robson, *Angew. Chem. Int. Ed.*, 1998, **37**, 1460–1494.
65 D. N. Williams, K. A. Gold, T. R. P. Holoman, S. H. Ehrman and O. C. Wilson, *J. Nanopart. Res.*, 2006, **8**, 749–753.
66 C. Aschkenasy and J. Kost, *J. Control. Release*, 2005, **110**, 58–66.
67 L. F. Scatena, M. G. Brown and G. L. Richmond, *Science*, 2001, **292**, 908–912.
68 S. K. Smoukov, K. J. M. Bishop, B. Kowalczyk, A. M. Kalsin and B. A. Grzybowski, *J. Am. Chem. Soc.*, 2007, **129**, 15623–15630.
69 A. M. Kalsin and B. A. Grzybowski, *Nano Lett.*, 2007, **7**, 1018–1021.
70 K. J. M. Bishop and B. A. Grzybowski, *ChemPhysChem*, 2007, **8**, 2171–2176.
71 S. Y. Park, A. K. R. Lytton-Jean, B. Lee, S. Weigand, G. C. Schatz and C. A. Mirkin, *Nature*, 2008, **451**, 553–556.
72 D. N. Chin, G. T. R. Palmore and G. M. Whitesides, *J. Am. Chem. Soc.*, 1999, **121**, 2115–2122.
73 A. Marsh, M. Silvestri and J. M. Lehn, *Chem. Commun.*, 1996, 1527–1528.
74 J. A. Zerkowski, J. C. Macdonald and G. M. Whitesides, *Chem. Mat.*, 1994, **6**, 1250–1257.
75 J. M. Lehn, *Supramolecular Chemistry: Concepts and Perspectives*, Wiley-VCH, New York, 1995.
76 Y. S. Velichko, S. I. Stupp and M. O. de la Cruz, *J. Phys. Chem. B*, 2008, **112**, 2326–2334.
77 K. Rajangam, H. A. Behanna, M. J. Hui, X. Q. Han, J. F. Hulvat, J. W. Lomasney and S. I. Stupp, *Nano Lett.*, 2006, **6**, 2086–2090.
78 V. M. Tysseling-Mattiace, V. Sahni, K. L. Niece, D. Birch, C. Czeisler, M. G. Fehlings, S. I. Stupp and J. A. Kessler, *J. Neurosci.*, 2008, **28**, 3814–3823.
79 E. V. Shevchenko, D. V. Talapin, N. A. Kotov, S. O'Brien and C. B. Murray, *Nature*, 2006, **439**, 55–59.
80 A. van Blaaderen, R. Ruel and P. Wiltzius, *Nature*, 1997, **385**, 321–324.
81 S. O. Kim, H. H. Solak, M. P. Stoykovich, N. J. Ferrier, J. J. de Pablo and P. F. Nealey, *Nature*, 2003, **424**, 411–414.
82 M. P. Stoykovich, M. Muller, S. O. Kim, H. H. Solak, E. W. Edwards, J. J. de Pablo and P. F. Nealey, *Science*, 2005, **308**, 1442–1446.
83 J. Y. Cheng, A. M. Mayes and C. A. Ross, *Nat. Mater.*, 2004, **3**, 823–828.
84 J. Y. Cheng, F. Zhang, V. P. Chuang, A. M. Mayes and C. A. Ross, *Nano Lett.*, 2006, **6**, 2099–2103.
85 J. Y. Cheng, C. A. Ross, H. I. Smith and E. L. Thomas, *Adv. Mater.*, 2006, **18**, 2505–2521.
86 J. Aizenberg, A. J. Black and G. M. Whitesides, *Nature*, 1999, **398**, 495–498.
87 J. D. Le, Y. Pinto, N. C. Seeman, K. Musier-Forsyth, T. A. Taton and R. A. Kiehl, *Nano Lett.*, 2004, **4**, 2343–2347.
88 H. Y. Li, S. H. Park, J. H. Reif, T. H. LaBean and H. Yan, *J. Am. Chem. Soc.*, 2004, **126**, 418–419.
89 H. Yan, S. H. Park, G. Finkelstein, J. H. Reif and T. H. LaBean, *Science*, 2003, **301**, 1882–1884.
90 E. Braun, Y. Eichen, U. Sivan and G. Ben-Yoseph, *Nature*, 1998, **391**, 775–778.
91 S. Pruneanu, S. A. F. Al-Said, L. Q. Dong, T. A. Hollis, M. A. Galindo, N. G. Wright, A. Houlton and B. R. Horrocks, *Adv. Funct. Mater.*, 2008, **18**, 2444–2454.
92 Y. Shao, Y. D. Jin and S. J. Dong, *Electrochem. Commun.*, 2002, **4**, 773–779.
93 Y. M. Sun, M. Steinhart, D. Zschech, R. Adhikari, G. H. Michler and U. Gosele, *Macromol. Rapid Commun.*, 2005, **26**, 369–375.
94 H. Xiang, K. Shin, T. Kim, S. I. Moon, T. J. McCarthy and T. P. Russell, *Macromolecules*, 2005, **38**, 1055–1056.
95 M. L. Ma, V. Krikorian, J. H. Yu, E. L. Thomas and G. C. Rutledge, *Nano Lett.*, 2006, **6**, 2969–2972.
96 B. Yu, P. C. Sun, T. C. Chen, Q. H. Jin, D. T. Ding, B. H. Li and A. C. Shi, *Phys. Rev. Lett.*, 2006, **96**, 4.
97 Y. Y. Wu, G. S. Cheng, K. Katsov, S. W. Sides, J. F. Wang, J. Tang, G. H. Fredrickson, M. Moskovits and G. D. Stucky, *Nat. Mater.*, 2004, **3**, 816–822.
98 V. N. Manoharan, M. T. Elsesser and D. J. Pine, *Science*, 2003, **301**, 483–487.
99 D. M. Kuncicky, K. Bose, K. D. Costa and O. D. Velev, *Chem. Mat.*, 2007, **19**, 141–143.
100 D. M. Kuncicky and O. D. Velev, *Langmuir*, 2008, **24**, 1371–1380.
101 G. S. Attard, J. C. Glyde and C. G. Goltner, *Nature*, 1995, **378**, 366–368.
102 J. S. Beck, J. C. Vartuli, W. J. Roth, M. E. Leonowicz, C. T. Kresge, K. D. Schmitt, C. T. W. Chu, D. H. Olson, E. W. Sheppard, S. B. McCullen, J. B. Higgins and J. L. Schlenker, *J. Am. Chem. Soc.*, 1992, **114**, 10834–10843.
103 J. L. Blin, A. Leonard and B. L. Su, *Chem. Mat.*, 2001, **13**, 3542–3553.
104 H. P. Lin and C. Y. Mou, *Accounts Chem. Res.*, 2002, **35**, 927–935.
105 W. A. Lopes and H. M. Jaeger, *Nature*, 2001, **414**, 735–738.
106 M. M. Burns, J. M. Fournier and J. A. Golovchenko, *Science*, 1990, **249**, 749–754.
107 A. P. Hynninen, J. H. J. Thijssen, E. C. M. Vermolen, M. Dijkstra and A. Van Blaaderen, *Nat. Mater.*, 2007, **6**, 202–205.
108 T. L. Morkved, M. Lu, A. M. Urbas, E. E. Ehrichs, H. M. Jaeger, P. Mansky and T. P. Russell, *Science*, 1996, **273**, 931–933.
109 T. Thurn-Albrecht, J. Schotter, C. A. Kastle, N. Emley, T. Shibauchi, L. Krusin-Elbaum, K. Guarini, C. T. Black, M. T. Tuominen and T. P. Russell, *Science*, 2000, **290**, 2126–2129.
110 D. E. Angelescu, J. H. Waller, D. H. Adamson, P. Deshpande, S. Y. Chou, R. A. Register and P. M. Chaikin, *Adv. Mater.*, 2004, **16**, 1736–1740.
111 Y. Sahoo, M. Cheon, S. Wang, H. Luo, E. P. Furlani and P. N. Prasad, *J. Phys. Chem. B*, 2004, **108**, 3380–3383.
112 L. E. Helseth, *Langmuir*, 2005, **21**, 7276–7279.
113 R. M. Amos, J. G. Rarity, P. R. Tapster, T. J. Shepherd and S. C. Kitson, *Phys. Rev. E*, 2000, **61**, 2929–2935.
114 M. Trau, D. A. Saville and I. A. Aksay, *Science*, 1996, **272**, 706–709.
115 B. A. Grzybowski, H. A. Stone and G. M. Whitesides, *Proc. Natl. Acad. Sci. USA*, 2002, **99**, 4147–4151.
116 B. A. Grzybowski, X. Y. Jiang, H. A. Stone and G. M. Whitesides, *Phys. Rev. E*, 2001, **64**, 011603.
117 G. Helgessen, E. Svasand and A. T. Skjeltorp, *J. Phys. Condens. Matter*, 2007, **20**, 204127.
118 M. R. Sawaya, S. Y. Guo, S. Tabor, C. C. Richardson and T. Ellenberger, *Cell*, 1999, **99**, 167–177.
119 T. M. Lohman and K. P. Bjornson, *Annu. Rev. Biochem.*, 1996, **65**, 169–214.
120 G. Y. Liu, S. Xu and Y. L. Qian, *Accounts Chem. Res.*, 2000, **33**, 457–466.
121 D. J. Timson, M. R. Singleton and D. B. Wigley, *Mutat. Res.-DNA Repair*, 2000, **460**, 301–318.

122 B. Alberts, A. Johnson, J. Lewis, M. Raff, K. Roberts and P. Walter, *Molecular Biology of The Cell*- 4th ed., Garland Science, New York, 2002.
123 T. D. Pollard, *Nature*, 2003, **422**, 741–745.
124 H. P. Erickson and E. T. Obrien, *Annu. Rev. Biophys. Biomolec. Struct.*, 1992, **21**, 145–166.
125 T. Wittmann, A. Hyman and A. Desai, *Nat. Cell Biol.*, 2001, **3**, E28–E34.
126 E. Ben-Jacob, I. Cohen and D. L. Gutnick, *Annu. Rev. Microbiol.*, 1998, **52**, 779–806.
127 E. Ben-Jacob, I. Cohen and H. Levine, *Adv. Phys.*, 2000, **49**, 395–554.
128 G. Nicolis and I. Prigogine, *Self-Organization in Nonequilibrium Systems: From Dissipative Structures to Order Through Fluctuations*, John Wiley & Sons, New York, 1977.
129 S. R. de Groot and P. Mazur, *Nonequilibrium Thermodynamics*, Dover Publications, New York, 1984.
130 H. G. Schuster, *Deterministic Chaos: An Introduction*, Wiley-VCH, Deerfield Beach, 1984.
131 D. J. Evans and G. P. Morriss, *Statistical Mechanics of Nonequilibrium Liquids*, Academic Press, London; San Diego, 1990.
132 J. R. Dorfman, *An Introduction to Chaos in Nonequilibrium Statistical Mechanics*, Cambridge University Press, New York, 1999.
133 D. J. Evans and A. Baranyai, *Phys. Rev. Lett.*, 1991, **67**, 2597–2600.
134 W. G. Hoover, *Computational Statistical Mechanics*, Elsevier, New York, 1991.
135 W. G. Hoover and H. A. Posch, *Phys. Rev. E*, 1994, **49**, 1913–1920.
136 S. Sasa and T. S. Komatsu, *Phys. Rev. Lett.*, 1999, **82**, 912–915.
137 W. G. Breymann, T. Tel and J. Vollmer, *Phys. Rev. Lett.*, 1996, **77**, 2945–2948.
138 M. E. Tuckerman, C. J. Mundy and M. L. Klein, *Phys. Rev. Lett.*, 1997, **78**, 2042–2045.
139 P. Gaspard and G. Nicolis, *Phys. Rev. Lett.*, 1990, **65**, 1693–1696.
140 J. Vollmer, T. Tel and W. Breymann, *Phys. Rev. Lett.*, 1997, **79**, 2759–2762.
141 C. Jarzynski, *Phys. Rev. Lett.*, 1997, **78**, 2690–2693.
142 C. Jarzynski, *Phys. Rev. E*, 1997, **56**, 5018–5035.
143 G. E. Crooks, *Phys. Rev. E*, 2000, **61**, 2361–2366.
144 J. Kurchan, *J. Stat. Mech: Theory Exp.*, 2007, P07005.
145 J. D. Farmer, E. Ott and J. A. Yorke, *Physica D*, 1983, **7**, 153–180.
146 M. Fialkowski, K. J. M. Bishop, R. Klajn, S. K. Smoukov, C. J. Campbell and B. A. Grzybowski, *J. Phys. Chem. B*, 2006, **110**, 2482–2496.
147 B. A. Grzybowski and C. J. Campbell, *Chem. Eng. Sci.*, 2004, **59**, 1667–1676.
148 B. A. Grzybowski and G. M. Whitesides, *J. Phys. Chem. B*, 2001, **105**, 8770–8775.
149 B. A. Grzybowski and G. M. Whitesides, *J. Chem. Phys.*, 2002, **115**, 8571–8577.
150 S. Soh, K. J. M. Bishop and B. A. Grzybowski, *J. Phys. Chem. B*, 2008, **112**, 10848–10853.
151 S. Nakata and Y. Hayashima, *J. Chem. Soc. Faraday Trans.*, 1998, **94**, 3655–3658.
152 L. Rayleigh, *Proc. R. Soc. London*, 1890, **47**, 364–367.
153 P. R. Ashton, R. Ballardini, V. Balzani, I. Baxter, A. Credi, M. C. T. Fyfe, M. T. Gandolfi, M. Gomez-Lopez, M.-V. Martinez-Díaz, A. Piersanti, N. Spencer, J. F. Stoddart, M. Venturi, A. J. P. White and D. J. Williams, *J. Am. Chem. Soc.*, 1998, **120**, 11932–11942.
154 C. P. Collier, G. Mattersteig, E. W. Wong, Y. Luo, K. Beverly, J. Sampaio, F. M. Raymo, J. F. Stoddart and J. R. Heath, *Science*, 2000, **289**, 1172–1175.
155 J. Wu, K. C.-F. Leung, D. Benítez, J.-Y. Han, S. J. Cantrill, L. Fang and J. F. Stoddart, *Angew. Chem. Int. Ed.*, 2008, **47**, 7470–7474.
156 *Molecular Switches*, ed. B. L. FeringaWiley - VCH Weinheim, 2001.
157 R. Klajn, K. J. M. Bishop and B. A. Grzybowski, *Proc. Natl. Acad. Sci. USA*, 2007, **104**, 10305–10309.
158 I. R. Epstein and K. Showalter, *J. Phys. Chem.*, 1996, **100**, 13132–13147.
159 B. A. Grzybowski, K. J. M. Bishop, C. J. Campbell, M. Fialkowski and S. K. Smoukov, *Soft Matter*, 2005, **1**, 114–128.
160 K. J. M. Bishop, R. Klajn and B. A. Grzybowski, *Angew. Chem. Int. Ed.*, 2006, **45**, 5348–5354.
161 M. Fialkowski, K. J. M. Bishop, V. A. Chubukov, C. J. Campbell and B. A. Grzybowski, *Angew. Chem. Int. Ed.*, 2005, **44**, 7263–7269.
162 K. Kurin-Csorgei, I. R. Epstein and M. Orban, *Nature*, 2005, **433**, 139–142.
163 Z. Dogic and S. Fraden, *Phase Behavior of Rod-Like Viruses and Virus–Sphere Mixtures*, Wiley-VCH, Weinheim, 2006.
164 A. Nangia, *Accounts Chem. Res.*, 2008, **41**, 595–604.
165 J. Israelachvili, *Intermolecular & Surface Forces*, Academic Press, Amsterdam, 1991.
166 P. Bertrand, A. Jonas, A. Laschewsky and R. Legras, *Macromol. Rapid Commun.*, 2000, **21**, 319–348.
167 G. S. Bassi, N. E. Mollegaard, A. I. H. Murchie, E. Vonkitzing and D. M. J. Lilley, *Nat. Struct. Biol.*, 1995, **2**, 45–55.
168 C. A. Miller, J. P. Hernandez-Ortiz, N. L. Abbott, S. H. Gellman and J. J. de Pablo, *J. Chem. Phys.*, 2008, **129**, 10.
169 K. Isoda, T. Yasuda and T. Kato, *J. Mater. Chem.*, 2008, **18**, 4522–4528.
170 Y. H. Liu, Z. G. Li, L. J. Yang and X. L. Liu, *J. Chem. Crystallogr.*, 2008, **38**, 867–871.
171 S. I. Stupp, V. LeBonheur, K. Walker, L. S. Li, K. E. Huggins, M. Keser and A. Amstutz, *Science*, 1997, **276**, 384–389.
172 J. H. Ryu, D. J. Hong and M. Lee, *Chem. Commun.*, 2008, 1043–1054.
173 J. Lahiri, L. Isaacs, B. Grzybowski, J. D. Carbeck and G. M. Whitesides, *Langmuir*, 1999, **15**, 7186–7198.
174 H. W. Shen, L. F. Zhang and A. Eisenberg, *J. Am. Chem. Soc.*, 1999, **121**, 2728–2740.
175 K. Mitamura, T. Imae, N. Saito and O. Takai, *J. Phys. Chem. B*, 2007, **111**, 8891–8898.
176 H. Onoe, K. Matsumoto and I. Shimoyama, *Proceedings: IEEE Micro Electro Mechanical Systems Workshop,* 2003.
177 D. B. Wolfe, A. Snead, C. Mao, N. B. Bowden and G. M. Whitesides, *Langmuir*, 2003, **19**, 2206–2214.
178 D. Vella and L. Mahadevan, *Am. J. Phys.*, 2005, **73**, 817–825.
179 D. J. Klingenberg, J. C. Ulicny and A. Smith, *Appl. Phys. Lett.*, 2005, 86.
180 Y. Kasai and Y. Morimoto, *International Congress on Transportation Electronics*, Dearborn, MI, USA, 1988.
181 W. I. Kordonski and D. Golini, *J. Intell. Mater. Syst. Struct.*, 2000, **10**, 683–689.
182 J. D. Carlson, W. Matthis and J. R. Toscano, Smart prosthetics based on magnetorheological fluids, in *Smart Structures and Materials 2001. Industrial and Commercial Applications of Smart Structures Technologies*, SPIE, Bellingham, Washington, 2001.
183 M. S. Cho, S. B. Choi and N. M. Wereley, *Int. J. Mod. Phys. B*, 2005, **19**, 1696–1702.
184 M. J. Chrzan and J. D. Carlson, MR fluid sponge devices and their use in vibration control of washing machines, in *Smart Structures and Materials 2001. Damping and Isolation,* SPIE, Bellingham, Washington, 2001.
185 W. J. Wen, L. Y. Zhang and P. Sheng, *Phys. Rev. Lett.*, 2000, **85**, 5464–5467.
186 W. Wen and P. Sheng, *Physica B*, 2003, **338**, 343–346.
187 B. F. Spencer and M. K. Sain, *IEEE Control Syst. Mag.*, 1997, **17**, 19–35.
188 S. J. Dyke, B. F. Spencer, M. K. Sain and J. D. Carlson, *Smart Mater. Struct.*, 1998, **7**, 693–703.
189 S. J. Dyke, B. F. J. Spencer, M. K. Sain and J. D. Carlson, *Proceedings of the 1997 15th Structures Congress. Part 2*, Portland, OR, 1997.
190 S. Sahasrabudhe and S. Nagarajaiah, *J. Struct. Eng. ASCE*, 2005, **131**, 1025–1034.
191 S. S. Sahasrabudhe and S. Nagarajaiah, *Earthq. Eng. Struct. Dyn.*, 2005, **34**, 965–983.
192 B. F. Spencer and S. Nagarajaiah, *J. Struct. Eng. ASCE*, 2003, **129**, 845–856.
193 M. M. Burns, J. M. Fournier and J. A. Golovchenko, *Phys. Rev. Lett.*, 1989, **63**, 1233–1236.
194 J. M. K. Ng, M. J. Fuerstman, B. A. Grzybowski, H. A. Stone and G. M. Whitesides, *J. Am. Chem. Soc.*, 2003, **125**, 7948–7958.
195 P. Lenz, J. F. Joanny, F. Julicher and J. Prost, *Phys. Rev. Lett.*, 2003, **91**, 108104.
196 K. S. Fine, A. C. Cass, W. G. Flynn and C. F. Driscoll, *Phys. Rev. Lett.*, 1995, **75**, 3277–3280.
197 D. A. Schecter, D. H. E. Dubin, K. S. Fine and C. F. Driscoll, *Phys. Fluids*, 1999, **11**, 905–914.
198 J. Vermant and M. J. Solomon, *J. Phys. Condes. Matter*, 2005, **17**, R187–R216.

199 B. A. Grzybowski and G. M. Whitesides, *J. Phys. Chem. B*, 2002, **106**, 1188–1194.
200 Y. Hayashima, M. Nagayama and S. Nakata, *J. Phys. Chem. B*, 2001, **105**, 5353–5357.
201 S. Nakata, M. I. Kohira and Y. Hayashima, *Chem. Phys. Lett.*, 2000, **322**, 419–423.
202 M. I. Kohira, Y. Hayashima, M. Nagayama and S. Nakata, *Langmuir*, 2001, **17**, 7124–7129.
203 M. Parthasarathy and D. J. Klingenberg, *Mater. Sci. Eng. R-Rep.*, 1996, **17**, 57–103.
204 W. D. Ristenpart, I. A. Aksay and D. A. Saville, *Phys. Rev. Lett.*, 2003, **90**, 128303.
205 S. Sohn, Writing method for ink jet printer using electro-rheological fluid and apparatus thereof, U.S. Patent 994 908, 1996.
206 X. Wen, Ink jet printing apparatus and method using timing control of electronic waveforms for variable gray scale printing without artifacts, U.S. Patent 928 003, 2000.
207 R. W. Gundlach and E. G. Rawson, Electrorheological based droplet ejecting printer. U.S. Patent 140 658, 2000.
208 Y. Akagami, K. Asari, B. Jeyadevan and T. Fujita, *J. Intell. Mater. Syst. Struct.*, 1999, **9**, 672–675.
209 Y. Akagami, K. Asari, B. Jeyadevan, T. Fujita and N. Umehara, *J. Intell. Mater. Syst. Struct.*, 2000, **10**, 753–756.
210 P. M. Taylor, D. M. Pollet, A. Hosseini-Sianaki and C. J. Varley, *Displays*, 1998, **18**, 135–141.
211 C. Mavroidis, *Res. Nondestruct. Eval.*, 2002, **14**, 1–32.
212 M. V. Sapozhnikov, Y. V. Tolmachev, I. S. Aranson and W. K. Kwok, *Phys. Rev. Lett.*, 2003, **90**, 114301.
213 I. S. Aranson and M. V. Sapozhnikov, *Phys. Rev. Lett.*, 2004, **92**, 234301.
214 G. Albrecht-Buehler, *Proc. Natl. Acad. Sci. USA*, 2005, **102**, 5050–5055.
215 B. Hoffmann and W. Kohler, *J. Magn. Magn. Mater.*, 2003, **262**, 289–293.
216 R. R. Kellner and W. Kohler, *J. Appl. Phys.*, 2005, **97**, 034910.